

Young Belgian Magnetic Resonance Scientist 2025

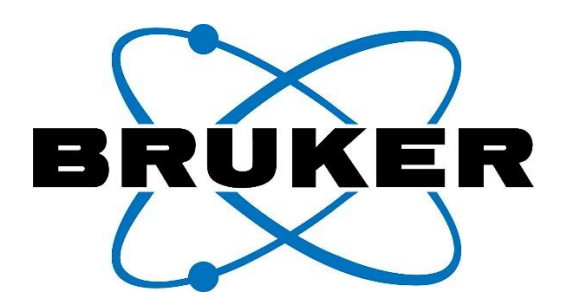
Program Book

21th edition of YBMRS

November 6^h-7th 2025

Floréal, Blankenberge

Platinum Sponsor



Gold Sponsor

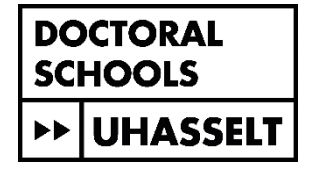


With the support of





















Symposium Program

Thursday, 6th November – Day 1

09:00 - Registration and Poster Setup

10:00 - Welcome

Educational Session 1

Chair: Dr. Elien Derveaux

10:10 - Tutorial: "Decoding modern NMR methods to unlock their full potential" Prof. Laura

Castanar-Acedo

11:05 - Tutorial: "What can and cannot be simulated in Magnetic Resonance" Prof. Ilya Kuprov

12:00 - Lunch

Plenary Session 1

Chair: Dr. Luca Fusaro

13:00 - **Invited Speaker:** *Prof. Laura Castanar-Acedo* (Universidad Complutense de Madrid)

Simplifying complexity: novel NMR tools to aid spectral analysis

Chair: Dr. Roy Lavendomme

13:50 - 3D printing of subject-specific passive shims to improve in vivo MRI - A. Vanduffel

14:10 - Synthesis and optimisation of gallium-doped dendritic silica materials for CO₂

conversion: a structure-activity correlation via ssNMR - N. Pierard

14:30 - Flash Presentations of Posters

14:50 - Poster Session 1 & Coffee Break (1h30)

Plenary Session 2

Chair: Prof. José Martins

16:20 - Invited Speaker: Prof. Ilya Kuprov (Weizmann Institute, Rehovot) Deep neural networks

in magnetic resonance data processing

Chair: Dr. Ewoud Vaneeckhaute

17:10 - ¹H-NMR metabolomics of cocoa beans and derived cocoa liquors and chocolates after spontaneous or starter culture-initiated fermentation - E. Tuenter

17:30 - Integrating NMR and dielectric spectroscopy in a single multi-diagnostic probe-head for the investigation of nanoconfined water - A. F. Morais

17:50 - Monte Carlo study of high-field transverse relaxation induced by iron oxide nanoparticles coated by a slow water diffusion layer - E. Martin

18:10 - End of Session

18:30–19:00 - General Assembly

19:00 - Reception & Networking - followed by Dinner

Friday, 7th November – Day 2

Educational Session 2

Chair: Dr. Anthony Morena

09:00 - **Tutorial:** "Understanding Quadrupolar Nuclei in Solid-State NMR: From Theory to Practical Aspects" – Prof. Laurent Delevoye

09:55 - Cracking MOF secrets with NMR crystallography: Isoreticular expansion in porous Al(III) and Ga(III) phosphonates - *J. Theissen*

10:15 - Poster Session 2 & Coffee Break (1h30)

Plenary Session 3

Chair: Dr. Yoanes Maria Vianney

11:45 - Hyperpolarized protic solvents as a general resource for polarization transfer - *E. Vaneeckhaute*

12:05 - Silica-based nanotubes and nanospheres: versatile materials from micellization studies to greener pathways - *V. Marsala*

12:25 - Unlocking homonuclear geminal couplings for conformational analysis of flexible molecules - *E. Norzagaray*

12:45 - Multi-harmonic EPR detection of melanin in skin melanomas: from mice to men - *M*. *Wehbi*

13:05 - Lunch & Group Photo

Plenary Session 4

Chair: Prof. Peter Adriaensens

14:30 - **Invited Speaker:** *Prof. Laurent Delevoye* (Université de Lille / CNRS) *Structure—activity relationships in catalysts with advanced solid-state NMR of quadrupolar nuclei*

Chair: Prof. Peter Adriaensens

15:20 - Unravelling competitive adsorption in zeolites with solid-state NMR - *S. Radhakrishnan* **15:40** - Mapping cancer's metabolic footprint: plasma NMR for early NSCLC diagnosis - *J. Meynen*

16:00 - Solution-state NMR spectroscopic characterization of metal—organic assemblies - *R. Lavendomme*

16:20 - Coffee Break

16:50 - Awards and Closing Remarks

17:10 - End of Symposium

The book of abstracts can be downloaded on the conference website: www.ybmrs.be

ABSTRACTS TUTORIALS AND PLENARY LECTURES

YBMRS 25 – November 2025 – Floréal Blankenberge

Decoding modern NMR methods to unlock their full potential

Laura Castanar-Acedo

Universidad Complutense de Madrid

To be announced

YBMRS 25 – November 2025 – Floréal Blankenberge

What can and cannot be simulated in Magnetic Resonance

Ilya Kuprov

Department of Chemical and Biological Physics, Weizmann Institute of Science, Israel

Numerical simulation and fitting can save a lot of time by answering basic questions about a magnetic resonance experiment: "Is this realistic?", "What are the optimal parameters?", "Would the data answer my question?", "What the hell just happened?", etc. Particularly the latter. A significant fraction of collaborative work in any theory group is assisting chemists who run into the weirdest NMR spectrum they have ever seen, google it up, find a PDF with twenty pages of equations, and think "oookaay... let's see if those nerds on the seventh floor are as useful as they claim to be." Well, we try. This tutorial will provide an overview of modern magnetic resonance simulation capabilities and explain how we run simulations, what can be simulated, what cannot, and why.

Understanding Quadrupolar Nuclei in Solid-State NMR: From Theory to Practical Aspects

L. Delevoye¹

¹ Unité de Catalyse et Chimie du Solide (UCCS), UMR 8181, Univ. Lille, CNRS, Centrale Lille, Univ. Artois, Lille 59000, France.

Solid-state NMR is a powerful technique to probe the local order and disorder in a wide range of materials, offering molecular-scale insight through the interactions it reveals. Unlike diffraction-based methods that average over long-range periodicity, NMR is sensitive to the local chemical environment, making it essential for characterizing amorphous phases, defects, and surface species. Among the many nuclei with non-zero spin, quadrupolar nuclei, those with spin greater than ½, represent nearly 75% of all NMR-active isotopes. They include key elements such as ¹7O, ²7AI, ²3Na, 95Mo, or 93Nb (and many others), which play a central role in determining the structural and functional properties of materials. Their study is therefore essential for understanding and optimizing systems, from inorganic solids to catalytic interfaces.

This tutorial will provide a short but comprehensive introduction to the principles and practical aspects of solid-state NMR spectroscopy for half-integer quadrupolar nuclei. We will begin with a brief theoretical overview of the key interactions in solids, with particular attention to the effects of anisotropy in powder samples. The session will then focus on the distinctive features of quadrupolar nuclei, highlighting how their behavior differs from "spin-1/2" systems. Parameters such as the quadrupolar coupling constant (C_Q) and asymmetry parameter (η_Q) will be defined, along with their spectral features and structural implications.

We will then explore the technical strategies developed to suppress, reintroduce, or exploit quadrupolar interactions, including pulse sequences and hardware advances. A large part of the tutorial will be dedicated to experimental methodologies that have emerged over the past decades to enhance sensitivity, achieve high-resolution spectra of half-integer quadrupolar nuclei, and access heteronuclear correlations. These techniques will be illustrated through examples drawn from diverse domains of applications, ranging from solid-state materials to heterogeneous catalysis.

By the end of the session, participants will have acquired an expanded methodological toolbox to address structural questions through the observation of quadrupolar nuclei in solid-state NMR spectroscopy.

YBMRS 25 – November 2025 – Floréal Blankenberge

Simplifying complexity: novel NMR tools to aid spectral analysis <u>Laura Castanar-Acedo</u>

Universidad Complutense de Madrid

To be announced

.

YBMRS 25 – November 2025 – Floréal Blankenberge

Deep neural networks in magnetic resonance data processing

Ilya Kuprov

Department of Chemical and Biological Physics, Weizmann Institute of Science, Israel

This lecture provides an overview of the recent results in magnetic resonance data processing using machine learning methods and reports some of our recent work in this area.

At the time of writing, the most impressive applications are in what mathematicians call "ill-posed problems": situations where the answer is not fully constrained by the input and / or depends very strongly on tiny perturbations therein.

Examples include inverse Laplace transform processing of DOSY data, inter-electron distance distribution extraction from DEER data, sparsely sampled NMR spectrum reconstruction, virtual decoupling of protein NMR spectra, peak picking and peak probability representations, resolution enhancement, *etc.*

In all these cases, neural networks vastly exceed expectations on performance; the reasons are still not well understood. This lecture will discuss the current state of that art as applied to nuclear and electron spin resonance.

Structure-activity relationships in catalysts with advanced solid-state NMR of quadrupolar nuclei

M. Taoufik, 1 R. M. Gauvin, 2 L. Delevoye2

Solid-state NMR spectroscopy has become a central technique for probing the local environments of catalytic materials, offering unparalleled insight into structure—activity relationships. Complementary to traditional characterization methods such as X-ray diffraction, electron microscopy, and vibrational spectroscopy, and in many cases surpassing them in sensitivity to local disorder and chemical heterogeneity, solid-state NMR provides a unique powerful framework into the atomic-scale structure of catalysts. This is especially true for quadrupolar nuclei, which constitute over 75% of NMR-active isotopes and are omnipresent in catalytically relevant systems, from zeolites and metal oxides to organometallic complexes. Recent methodological advances, including ultra-high magnetic fields and sophisticated pulse sequences, have dramatically enhanced resolution and sensitivity, enabling the detailed characterization of complex, disordered, and multi-component catalytic materials. Together, these developments make solid-state NMR an indispensable tool in the rational design and mechanistic understanding of catalytic systems.

This keynote will highlight recent advances in the characterization of catalytic materials through quadrupolar solid-state NMR, focusing on nuclei central to both inorganic-support structure and active site environment. For example, the structure of γ-alumina, a widely used support, is revisited using high-resolution ²⁷Al and ¹H NMR correlation experiments to unravel the distribution of surface hydroxyl sites.[1] For silica-supported systems, ¹⁷O NMR proves essential in distinguishing grafting modes and elucidating the local geometry of surface-bound species.[2] Recent developments in ⁹⁵Mo MAS NMR have enabled, for the first time, direct observation of the first coordination sphere of molybdenum centers in heterogeneous catalysts. This experimental work is conducted in close connexion with theoretical chemistry approaches, allowing us to probe the electronic and structural impact of ligands on the Mo center and to correlate NMR to computed parameters. These studies are further empowered by the advent of ultra-high magnetic fields, such as the 28.2 T spectrometer now operational in Lille, which allow access to nuclei with extremely large quadrupolar couplings and open new avenues for resolving complex local environments previously inaccessible to NMR.[3]

- 1. Merle, N., Tabassum, T., Scott, S., Motta, A., Szeto, K., Taoufik, M., Gauvin, R. M., Delevoye, L. *Angew. Chem. Int. Ed.* 2022, **61**, e202207316.
- 2. Merle, N., Trébosc, J., Baudouin, A., Del Rosal, I., Maron, L., Szeto, K., Genelot, M., Mortreux, A., Taoufik, M., Delevoye, L., Gauvin, R. M. *J. Am. Chem. Soc.* 2012, **134**, 9263-9275.
- 3. Szeto, K., Taoufik, M., Fayon, F., Gajan, D., Zurek, E., Autschbach, J., Trébosc, J., Delevoye, L., Gauvin, R. M. *Angew. Chem. Int. Ed.* 2025, **64**, e202508409.

¹ Laboratoire de Catalyse Polymérisation Procédés et Matériaux (CP2M), CNRS UMR 5128, Univ. Lyon1, CPE Lyon, Université de Lyon, Villeurbanne F-69616, France.

² Institut de Recherche de Chimie Paris, Chimie Paris Tech, PSL University, CNRS, 11 rue Pierre et Marie Curie, Paris 75005, France.

³ Unité de Catalyse et Chimie du Solide (UCCS), UMR 8181, Univ. Lille, CNRS, Centrale Lille, Univ. Artois, Lille 59000, France.

YBMRS 25 – November 2025 – Floréal Blankenberge

ABSTRACTS ORAL CONTRIBUTIONS

3D printing of subject-specific passive shims to improve in vivo MRI

A. Vanduffel(1), H. Vanduffel(1), C. Parra(1), Q. Goudard(1), U. Himmelreich(2), D. Sakellariou(1), R. Ameloot(1)

(1) cMACS, KU Leuven

(2) MOSAIC, KU Leuven

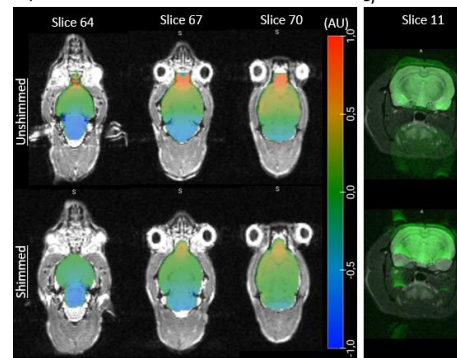
Introduction: Magnetic resonance imaging (MRI) depends on a highly uniform magnetic field (B₀) to achieve optimal image quality. However, patient-specific anatomical features and medical implants introduce local B₀ inhomogeneities, which compromise imaging performance^[1]. To mitigate these effects, Bo can be adjusted, or "shimmed," to improve uniformity. Passive shimming strategically places magnetizable materials to enhance field uniformity^[2]. However, passive shimming has seen limited use for correcting subject-induced B₀ variations, largely due to its labor-intensive nature, high costs, and difficulties in addressing higher-order field distortions^[3].

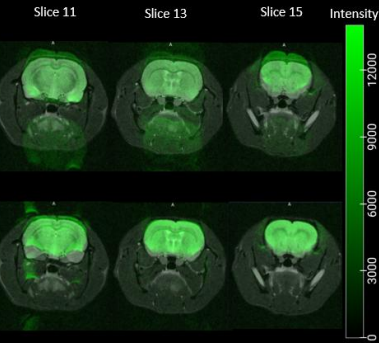
This research introduces a novel 3D printing approach to fabricate customized passive shims aimed at correcting in vivo field inhomogeneities. Unlike conventional methods, our powder-binder jetting technology allows efficient production of shims with intricate geometries without additional costs or extended fabrication times by allowing precise deposition of ferromagnetic material, generating higherorder spherical harmonic terms to optimize B₀ homogeneity^[4].

Methods: Field maps of female Fischer rats were acquired on a 9.4T animal MRI scanner (Fig. 1A). These maps served as input for a custom-developed shimming algorithm (MATLAB) designed to minimize the standard deviation of B₀ by employing the MEIGO global optimization toolbox^[5]. The concentration of ferromagnetic ink in each voxel to achieve optimal homogeneity was calculated and

converted into a grayscale printable CAD design. The design was fabricated via a modified powder-binder 3D printer.

Results: Simulations were performed for the brain as a region of interest (ROI). The standard deviations of both unshimmed and shimmed fields were compared. The results of the simulation demonstrated a potential improvement of 29% in B₀ field homogeneity. After printing and measuring the field maps with and without shim, an actual improvement $Figure\ 1\ (A)\ magnetic\ field\ maps\ before\ and\ after\ shimming.\ (B)\ EPI\ scan$ of 21% in standard deviation was observed





before and after shimming.

(Fig. 1A). This difference may arise from positioning variability in the scanner, noise during scanning, and printing imperfections. Additionally, EPI scans were taken to show the improvement after shimming (Fig. 1B).

Conclusion: Our results prove that 3D-printed passive shims can effectively homogenize the magnetic field in a scanner for in vivo species. Future research will focus on testing the technique on larger specimens (e.g., monkeys, dogs) and creating more generalized shims to further evaluate its efficacy.

- Yue-fen Zou, et al. (2015). Evaluation of MR issues for the latest standard brands of orthopedic metal implants: Plates and screws. European Journal of Radiology 84, p 450-457.
- Stockmann, J. P., & Wald, L. L. (2018). In vivo B0 field shimming methods for MRI at 7T. NeuroImage, 168, 71-87.
- Koch, K. M., et al. (2006). Sample-specific diamagnetic and paramagnetic passive shimming. Journal of magnetic resonance 182(1), p 66-74.
- Vanduffel et al. (2024). 3D printing of ferromagnetic passive shims for field shaping in magnetic resonance imaging. Journal of magnetic resonance, 363.
- 5. Egea, J.A., et al. (2014). MEIGO: an open-source software suite based on metaheuristics for global optimization in systems biology and bioinformatics. BMC Bioinformatics 15, p136.

Synthesis and Optimisation of Gallium Doped Dendritic Silica Materials for CO₂ Conversion: a Structure - Activity Correlation via ssNMR

N. Pierard₁, C. Célis₁, A. Morena₁, L. Fusaro₁, C. Aprile₁ 1 Laboratory of Applied Materials Chemistry, UCNANO, Department of Chemistry, Namur Institute of Structured Matter (NISM), University of Namur

In the context of green chemistry, the conversion of CO₂ into value-added products, such as cyclic carbonates (CC), is particularly attractive for the valorisation of this renewable source. However, the high stability of CO₂ requires the use of a catalyst that often displays both a nucleophilic and a Lewis (L) acid specie within the structure. In this regard, amorphous silicabased materials and in particular the newly developed dendritic one, are promising candidates as heterogeneous catalysts, due to their unique properties such as the easy surface functionalization and the possibility of inducing acidity in the final solid network via isomorphic substitution. In this context, the insertion of metal cations is particularly attractive, as they can provide both Brønsted (B) and Lewis acid sites both useful for the catalysis of CO₂ in CC₁. In this work, heterogeneous dendritic materials were synthetised choosing gallium as doping metal cation. Solid state nuclear magnetic resonance (ssNMR) played a fundamental role on analysing the insertion and the environment of the metal cation within the structure. The ssNMR of 71Ga of hydrated and dehydrated samples unveiled the correct insertion of the metal specie in the different solids synthetized by varying some synthesis parameters2. Moreover, the ssNMR technique coupled with trimethylphosphine (TMP) provided valuable insights into the nature of the acid sites present in the catalyst, including the Brønsted over Lewis ratio and the strength of the Lewis acid sites3. Since TMP alone cannot assess the strength of Brønsted acid sites, this information was obtained through a controlled oxidation of TMP to TMPO. Finally, the most promising material was tested as a catalyst in the reaction between CO₂ and epoxides to produce CC, demonstrating its efficiency for this reaction.

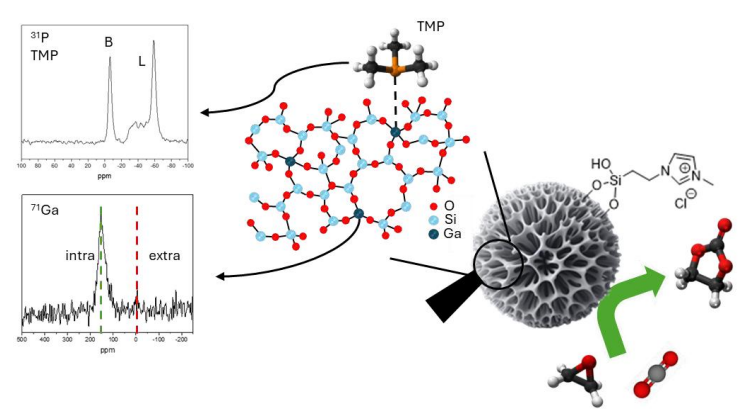


Figure 1: Bifunctional dendritic catalyst, illustrating gallium incorporation and acidity characterization by solid state NMR.

- 1. Célis, C., Armandi, M., Soumoy, L., Fiorilli, S., Aprile, C., Catalysis Today 2024, 429, 114467
- 2. Soumoy, L., Morena, A., Armandi, M., Fiorilli, S., Fusaro, L., Vivian, A., Debecker, D. P., Aprile, C., J. Catal. 2025, **447**, 116143.
- 3. Yi, X., Ko, H.-H., Deng, F., Liu, o S.-B., Zheng, A., Nat. Protoc. 2020, 15, 3527.

¹H-NMR metabolomics of cocoa beans and derived cocoa liquors and chocolates after spontaneous or starter culture-initiated cocoa fermentation

E. Tuenter¹, L. De Vuyst², K. Dewettinck³ and L. Pieters¹

Introduction: Cocoa and chocolate originate from the seeds of *Theobroma cacao* and are sources of various phytochemicals, like polyphenols, methylxanthines and biogenic amines, of which the flavan-3-ols in particular are associated with beneficial cardiovascular and cognitive effects. Processing of cocoa beans into chocolates involves several steps, like fermentation, roasting or conching, which can affect the levels of these phytochemicals. As for cocoa fermentation the use of starter cultures can aid in steering this process.²

Material & Methods: Phytochemicals in Trinitario cocoa beans from Costa Rica, harvested in 2019, were monitored during spontaneous and starter culture-initiated fermentation. The collected fresh and fermented cocoa beans, and derived cocoa liquors and chocolates were analyzed by ¹H-NMR spectroscopy, and multi-variate data analysis was applied.

Results: Cocoa beans could be distinguished according to fermentation degree, which was mainly driven by differences in signal intensities of signals corresponding to aliphatic amino acids and sucrose. While PCA (Principal Component Analysis) of the cocoa liquors still revealed segregation between the samples, the resulting chocolates clustered together, most probably due to a masking effect of sugar added to the cocoa liquors.

Conclusion: ¹H-NMR analysis of cocoa beans that underwent spontaneous or starter culture-initiated fermentation, as well as the resulting cocoa liquors, revealed that these samples could be distinguished according to fermentation degree. This method could therefore serve as alternative to the classic bean cut test, which involves visual inspection of the cocoa beans to assess their fermentation degree.

Supported by: Research Foundation Flanders (SBO project REVICO, S004617N).

- 1. V. Socci, D. Tempesta, G. Desideri, L. De Gennaro, M. Ferrara, Front. Nutr. 4, 19 (2017).
- 2.C. Díaz-Muñoz et al., Food Microbiology. 109, 104115 (2023).

¹Natural Products & Food Research and Analysis – Pharmaceutical Technology (NatuRAPT), Department of Pharmaceutical Sciences, University of Antwerp

²Research Group of Industrial Microbiology and Food Biotechnology (IMDO), Vrije Universiteit Brussel ³Food Structure & Function Research Group (FSF), Ghent University

Integrating NMR and dielectric spectroscopy in a single multi-diagnostic probehead for the investigation of nanoconfined water

<u>A. F. Morais</u>¹, S. Radhakrishnan¹, G. Arbiv^{1,2}, C. Vinod Chandran¹, J. A. Martens¹ and E. Breynaert^{1,2*}

Water is a polar molecule capable of forming strong hydrogen bonds, a feature that governs its properties and its role as a universal solvent. Nanoscale confinement disrupts the longrange hydrogen-bonding network of water, thus altering many of its known properties in the bulk state. Understanding the properties of nanoconfined water is essential for advancing our knowledge of biological, chemical and technological processes, including protein folding, solubility and catalytic activity. However, probing nanoconfined water remains challenging. No single technique can fully resolve the complexity of its hydrogen-bonding networks, necessitating the integration of multiple complementary methods, such as NMR and dielectric spectroscopy. Whereas NMR is focused to local atomic level characterization, allowing localization of nanoconfined molecules and investigation of short-range intermolecular interactions, dielectric spectroscopy yields information on the collective behaviour of dipolar fluctuations of the confined water phase. Although NMR and dielectric investigations of confined water systems are relatively abundant in the literature, the use of these techniques separately introduces its own difficulties to match and consistently interpret data acquired under the often-different experimental conditions imposed by each technique. For many samples, even small variations in conditions (pressure, temperature, water content, etc.) can

lead to markedly different behaviour. To enable simultaneous NMR and dielectric characterization to occur in a single setup, we demonstrate in this work a way to integrate dielectric spectroscopy in an NMR probe-head via the calibration of the magnitude of the probe-head detuning upon sample insertion.2 This method demands no hardware modification and is applicable to all probeheads subjected to frequency detuning. Using this tool, the molecular interactions and the dielectric properties of water confined in the micropores of MFI-type zeolites was characterized. Upon water uptake, the overall dielectric permittivity of the sample increases. An initial linear increase in permittivity similar to all MFI zeolites with different Si/Al ratios suggests a similar initial dielectric permittivity for water clusters in all zeolites, regardless of their surface polarity. Upon further increase in the water content, an inflection point is observed in the dielectric curves. This inflection point coincides with the maximum water uptake capacity of each zeolite from the gas phase and with the appearance of sharp ¹H NMR resonances indicative of the presence of mobile water in the systems. Asides confined water, the new in situ multi-diagnostic will also benefit the fields of battery research, food quality control and sensing, where both **NMR** and dielectric/impedance spectroscopy are common characterization techniques.

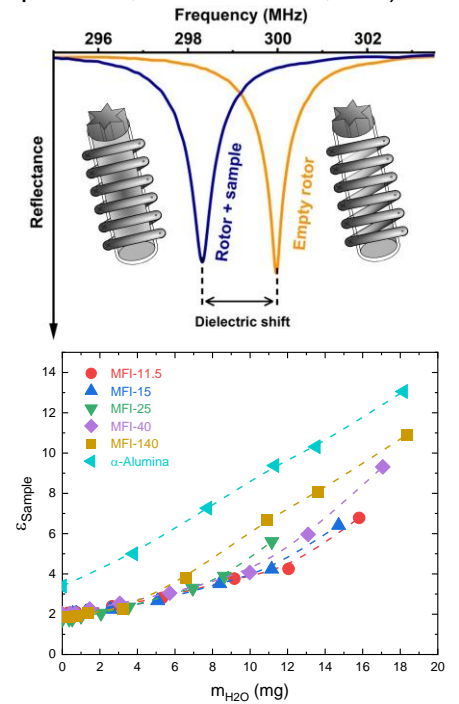


Figure 1. (Top) The magnitude of the probe detuning upon sample insertion – the dielectric shift – depends on the dielectric permittivity of the sample. (Bottom) The dielectric permittivity (at 500 MHz) of zeolite upon water addition.

- 1. E. Breynaert, M. Houlleberghs, S. Radhakrishnan, G. Grübel, F. Taulelle and J. A. Martens. Chem. Soc. Rev., 2020,49, 2557-2569
- 2. A. F. Morais, S. Radhakrishnan, G. Arbiv, D. Dom, K. Duerinckx, C. Vinod Chandran, J. A. Martens and E. Breynaert. Anal. Chem. 2024, 96, 13, 5071–5077

¹ NMR for Convergence Research (NMRCoRe), KU Leuven, Belgium

² Center for Molecular Water Science (CMWS), Hamburg, Germany

Monte Carlo study of high-field transverse relaxation induced by iron oxide nanoparticles coated by a slow water diffusion layer

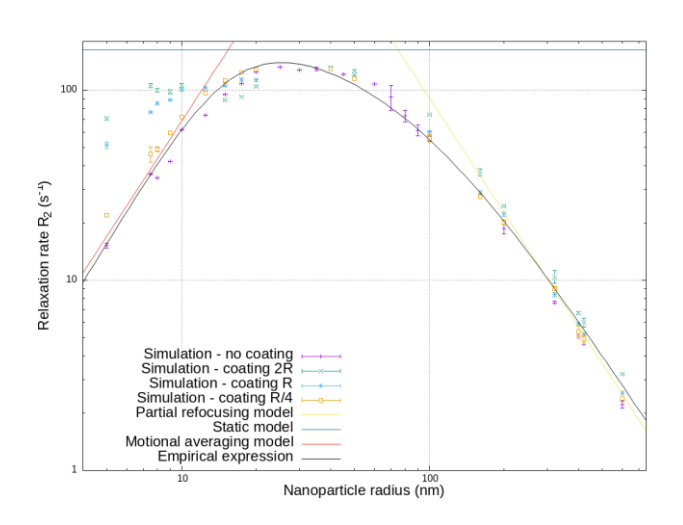
É. Martin¹, Y. Gossuin¹, Q.L. Vuong¹

Superparamagnetic iron oxide nanoparticles (SPIONs) are nanosize crystals of magnetite or maghemite. Their high saturation magnetisation and null remnant magnetisation make them particularly suitable to be used as contrast agents in nuclear magnetic resonance. Indeed, under the static magnetic fields typically used for NMR, they produce magnetic inhomogeneities, which modify the water relaxation rate where they are located. This in turn changes the pixel intensity in the area.

There is a variety of theoretical models that quantitatively predict the relaxation rate induced by such nanoparticles [1]. An important parameter is the diffusion coefficient of water molecules. However, these models only consider relaxation in a homogeneous medium, while SPIONs are usually coated with a layer of polymer. This coating is sometimes permeable to water and its water diffusion coefficient is usually smaller than that of bulk water. This inevitably affects the contrast induced by such nanoparticles [2]. Because they are complex to model analytically, numerical simulations are useful tools for studying the impact of these diffusion constraints on SPION-induced contrast.

This work hence aims at simulating, through Monte Carlo techniques, the influence of the nanoparticle polymer coating on SPION-induced T_2 NMR relaxation at high field. By varying the coating layer thickness and diffusion coefficient, it is shown that, especially with small SPIONs, thick coatings with slow diffusion lead to an increase in the water relaxation rate. This in turn leads to an increase in contrast. Our results indicate that efforts to produce thick coatings, permeable to water but with low diffusion coefficients, could improve the performance of SPIONs as contrast agents.

R (nm)	No coating	Thickness = R/4	Thickness = R	Thickness = 2R
	R ₂ (s ⁻¹)			
5	15.20 ± 0.45	22.04 ± 0.06	51.34 ± 2.04	70.9 ± 1.2
7.5	36.00 ± 0.30	46.0 ± 4.2	76.3 ± 0.8	105.2 ± 2.7
10	61.7 ± 0.7	72.3 ± 0.9	99.5 ± 1.5	105.8 ± 2.8
20	124.8 ± 1.7	128.5 ± 2.2	112.8 ± 2.3	104.2 ± 1.3
50	114.7 ± 0.9	129.0 ± 2.4	117.9 ± 3.2	125.8 ± 2.3
100	57.2 ± 3.4	55.6 ± 2.5	59.8 ± 1.7	74.1 ± 0.7
200	18.7 ± 1.2	20.1 ± 0.7	22.3 ± 0.6	24.55 ± 0.34
400	5.04 ± 0.10	5.39 ± 0.35	5.88 ± 0.11	6.73 ± 0.13
600	2.22 ± 0.10	2.392 ± 0.026	2.55 ± 0.05	3.219 ± 0.038



Simulated impact of the particle size and coating thickness on the relaxation rate induced by iron oxide nanoparticles. The diffusion coefficients in the solvent and in the coating are respectively $3 \cdot 10^{-9} \text{m}^2/\text{s}$ and $3 \cdot 10^{-10} \text{m}^2/\text{s}$. The magnetic volume fraction is $3.14 \cdot 10^{-6}$

- 1. Vuong Q.L., Gillis P. et al 2017 WIREs Nanomed Nanobiotechnol e1468 10.1002/wnan.1468
- 2. Peng Y., Li Y. et al 2023 Nanomed 54 10.1016/j.nano.2023.102713

¹ Biomedical Physics Unit, UMONS, Bâtiment 6, 25 Avenue Maistriau, 7000 Mons, Belgium

Cracking MOF secrets with NMR crystallography: Isoreticular Expansion in Porous Al(III) and Ga(III) Phosphonates: Synthesis, Structure, and Properties

<u>J. Theissen</u>^{1,2}, E. Derveaux², M. Radke³, R. Narvaez⁴, W. Marchal², P. Adriaensens², R. Ameloot¹, N. Stock³

Understanding the structure and chemistry of materials at the atomic scale is essential to rationalize their properties and unlock their application potential in future technologies. Metalorganic frameworks (MOFs), constructed from metal ions or clusters connected by organic linker molecules, represent a versatile class of porous materials.[1] While carboxylate- and imidazolate-based MOFs are well established, phosphonate MOFs and their isoreticular expansions remain comparatively underexplored. This is largely due to synthetic challenges and the complex coordination behaviour of phosphonic acids. [2]

In this study, we report a high-throughput investigation and **NMR crystallography** study of two new **phosphonate MOFs**, [M(OH)(H₂BPD)] (**M-CAU-67**, M = Al, Ga), synthesized in water under reflux conditions using the ditopic linker H₄BPD (N, N'-4,4'-bipiperidine-bis(methylenephosphonic acid)). Single-crystal X-ray diffraction, powder diffraction (PXRD), and complementary PDF analysis established the average framework connectivity. To resolve local structure and dynamics, we employed **solid-state MAS NMR spectroscopy** (²⁷**Al MQ-MAS**, ³¹**P MAS**), which provided key insights into coordination modes, hydrogen-bond interactions and dynamic flexibility of the network. These findings were further supported by simulations (Figure 1). The results highlight the structural responsiveness of CAU-67, which is isoreticular to the well-studied MOF MIL-91, but undergoes reversible transformations with temperature variation and water adsorption/desorption. By combining diffraction methods and solid-state NMR, this study provides a deeper structural understanding of M-CAU-67 and demonstrates the power of this combined approach for elucidating local coordination in complex phosphonate MOFs.

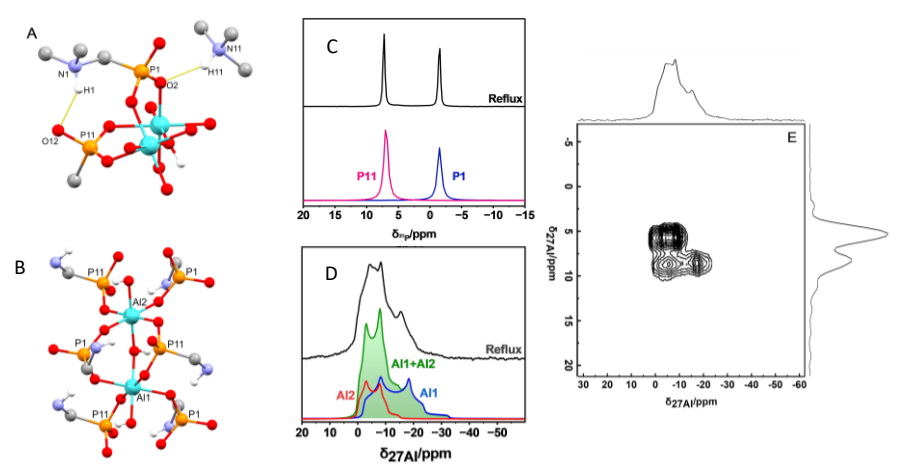


Figure 1: (A, B) Different coordination environments of Aluminum and Phosphorus in Al-CAU-67. (C) ³¹P MAS NMR spectrum of Al-CAU-67 (black) and simulation contributions of P1 (blue) and P11 (pink). (D) ²⁷Al MAS NMR spectrum of Al-CAU-67 (black) and simulation contributions of Al1 (blue), Al2 (red) and Al1 + Al2 (green). (E) ²⁷Al 3Q-MAS NMR spectrum of Al-CAU-67.

References

[1] G. Maurin et al. Chem. Soc. Rev. 46 (2017), 3104-3107.

[2] S. J. Shearan et al. Crystals. 9 (2019), 270.

¹ Center for membrane separations, adsorption, catalysis, and spectroscopy (cMACS), KULeuven.

² Institute for Materials Research (IMO-IMOMEC), Analytical and Circular Chemistry (ACC), NMR group, UHasselt.

³ Institut für Anorganische Chemie. Christian-Albrechts-Universität zu Kiel, Germany.

⁴ General Chemistry (ALGC) - Materials Modelling Group, Vrije Universiteit Brussel.

Hyperpolarized Protic Solvents as General Resource for Polarization Transfer

<u>Ewoud Vaneeckhaute^{1,2}</u>, Jean-Max Tyburn³, James G. Kempf⁴, Johan A. Martens^{1,2} and Eric Breynaert^{1,2}

Sensitivity poses a significant challenge in liquid-state nuclear magnetic resonance (NMR), often acting as a critical limitation. Parahydrogen (pH₂) offers a simple and repeatable means of boosting polarization, but its reliance on specific catalysts restricts its general use. [1] In contrast, dissolution dynamic nuclear polarization (dDNP) can generate larger molar polarization available to almost any analyte, yet requires the presence of relaxation-inducing radicals, cryogenic and microwave equipment, traditionally in a single-shot operation. [2] Addressing this gap requires a platform capable of producing large quantities of nuclear spin order that can serve as a general source of polarization. [3]

Here we show that protic solvents such as methanol/water mixtures could become a central element in such platform. In presence of ammonia, parahydrogen and a catalyst, protic solvents provide a reservoir of polarization, equivalent to polarizing the solvent at 80 T, but repeatedly produced at few millitesla through the signal amplification by reversible exchange (SABRE) method. This circumvents the overall need for large and expensive NMR magnets. Field-cycling analysis to an NMR spectrometer revealed a distinct transfer pathway to polarize 6 M of protons in the solvent: chemical exchange with labile protons from ammonia, until know only effective in more target-restrictive aprotic solvents such as dichloromethane, acetone, or chloroform. [4]

Further transfer to other molecules remains however difficult, and only dipolar-based cross-relaxation with pyridine aromatic protons is recognized but lacks efficiency. Further optimization on the solvent-solute transfer side is therefore needed to improve robustness and scalability to other analytes. Nonetheless, these results establish parahydrogen-based hyperpolarization routes as a repeatable and accessible route toward building a general polarization reservoir, opening possibilities for broader applications in chemistry, reaction monitoring and potentially imaging.

- [1] C. R. Bowers and D. P. Weitekamp, *J. Am. Chem. Soc.*, 1987, **109**, 5541–5542.
- [2] J. H. Ardenkjær-Larsen, B. Fridlund, A. Gram, G. Hansson, L. Hansson, M. H. Lerche, R. Servin, M. Thaning and K. Golman, *Proc. Natl. Acad. Sci.*, 2003, **100**, 10158–10163.
- [3] L. Dagys, M. C. Korzeczek, A. J. Parker, J. Eills, J. W. Blanchard, C. Bengs, M. H. Levitt, S. Knecht, I. Schwartz and M. B. Plenio, *Sci. Adv.*, 2024, **10**, eado0373.
- [4] E. Vaneeckhaute, J.-M. Tyburn, J. G. Kempf, J. A. Martens and E. Breynaert, *Chem. Commun.*, 2024, **60**, 13923–13926.

¹ NMRCoRe, NMR/X-Ray platform for Convergence Research, KULeuven, Celestijnenlaan 200F, box 2461, B-3001 Leuven, Belgium.

² COK-kat, Centre for Surface Chemistry and Catalysis – Characterisation and Application Team, KULeuven, Celestijnenlaan 200F, box 2461, B-3001, Belgium.

³ Bruker Biospin, 34 Rue de l'Industrie BP 10002, 67166 Wissembourg Cedex, France.

⁴ Bruker Biospin, 15 Fortune Dr., Billerica, 01821 Massachusetts, United States.

SILICA-BASED NANOTUBES AND NANOSPHERES: VERSATILE MATERIALS FROM MICELLIZATION STUDIES TO GREENER PATHWAYS

V. Marsala¹, N. Heydari¹, L. Fusaro^{1,*}, C. Aprile^{1,*}

¹ UCNANO, Department of Chemistry, NISM, University of Namur

In the past two decades, low-dimensional silica nanomaterials have emerged as versatile platforms for catalysis owing to their high surface area and tunable pore structures. Among them, hollow nanospheres (HNSs) and nanotubes (NTs) (Fig.1), synthesized through sol–gel chemistry and micelle-templated approaches, are particularly attractive.[1] Additionally, the isomorphic substitution of Si with metal cations allows creating acidic heterogeneous catalysts, hence opening the door to many catalytic applications.[2] Despite their potential, current synthetic routes present several environmental and time related limitations. Furthermore, when cations are introduced by co-synthesis, not all sites remain accessible. Finally, the morphological transition between HNSs and NTs is not yet fully understood.[3] In this work the micellization of the triblock copolymer Pluronic F127 has been investigated (Fig.1, right) by solution NMR (¹H, DQCOSY, NOESY), clarifying the pivotal role of toluene

(Fig.1, right) by solution NMR (¹H, DQCOSY, NOESY), clarifying the pivotal role of toluene concentration together with temperature. The NTs to HNSs transition was linked to the amount of toluene in the micelles, and room-temperature syntheses of pristine and Sn-doped HNSs confirmed that particle size can be tuned by adjusting temperature and swelling agent concentration.

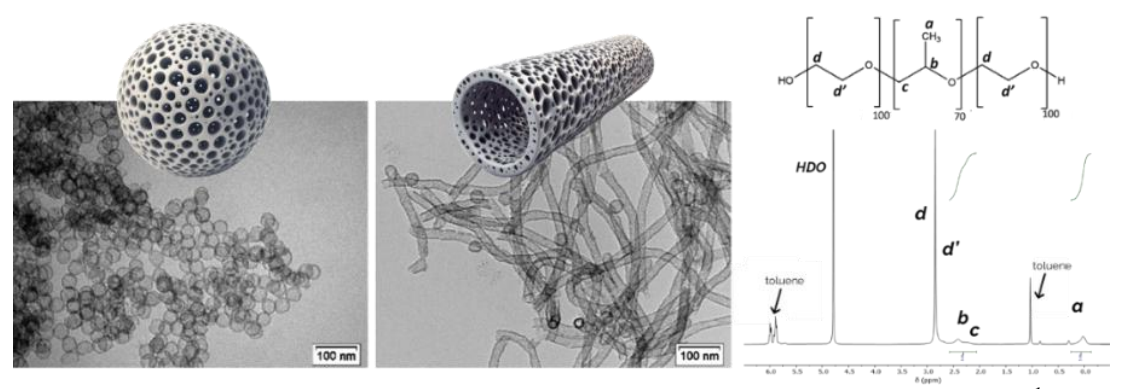


Figure 2. TEM micrographs of silica hollow nanospheres (left) and nanotubes (center); 1 H-NMR of Pluronic F127 ((PEO)₁₀₀(PPO)₇₀(PEO)₁₀₀) in the presence of toluene (right).

Moreover, co-synthetic and post-synthetic doping strategies were compared, and greener routes were explored, including room-temperature NT synthesis and time shortening *via* real-time monitoring of silica precursor hydrolysis by ¹H NMR. Finally, NTs were prepared incorporating tin, boron, aluminium, gallium, and indium cations, both as single dopants and in selected binary combinations. All the synthetised materials were characterized with SS-NMR of ²⁹Si, ¹¹⁹Sn, ²⁷Al, ⁷¹Ga. In particular, ²⁷Al SS-NMR enabled distinguishing tetrahedral, pentahedral, and octahedral Al environments and revealed a change in the intensity of some signals upon interaction with probe molecules such as water and acetone, thereby confirming the accessibility of framework sites together with the importance of hydration of samples for a correct analysis. All the materials were ultimately tested as heterogeneous catalysts for the conversion of glycerol into solketal, demonstrating their relevance in sustainable catalysis.

- [1] Huang, L., Kruk, M., Chem. Mater. 2015
- [2] Soumoy, L., Célis, C. Debecker, D.P., Armandi, M., Fiorilli S., Aprile, C., Journ. Cat. 2022
- [3] Soumoy, L., Fusaro, L., Debecker, D.P., Aprile, C., Chem. Mater. 2023

Unlocking homonuclear geminal couplings for conformational analysis of flexible molecules

E. Norzagaray^{1,2}, J.R.D. Montgomery^{1,2}, D. Sinnaeve^{1,2}

¹CNRS EMR 9002 — Integrative Structural Biology, F-59000 Lille, France ²Univ. Lille, Inserm, CHU Lille, Institut Pasteur de Lille, UMR 1167 — Risk Factors and Molecular Determinants of Aging-Related Diseases, F-59000 Lille, France

Scalar couplings (J) and especially residual dipolar couplings (RDCs) provide a wealth of information for the constitutional, configurational and conformational structure elucidation of organic compounds and biomacromolecules. [1,2] J-couplings depend on the electronic properties of molecular bonds between the nuclei, whereas RDCs report on both local and long-range molecular geometry, including the internuclear distance and the orientational properties of the internuclear vector between the nuclei. Within prochiral methylene (CH₂) moieties, the geminal ${}^2J_{HH}$ scalar coupling constants display some useful dependencies on local conformation.^[1] However, especially the two-bond ¹H-¹H RDC is attractive for structural analysis given their typically sizeable magnitudes and the fixed interproton distance. [2] The latter makes them especially interesting for the study of flexible molecules. Several experiments have been described that measure geminal ¹H-¹H couplings individually, but these only work well when the two proton multiplets are well-separated in the spectrum. [3-5] When the protons have similar chemical shifts and are strongly coupled and their multiplets appear to have 'merged', their extraction is challenging using frequency-selective methods. Recent selective J-resolved experiments based on ¹³C satellites equally cannot work for strongly coupled geminal ¹H-¹H couplings.^[6]

Here we present the 'Inverse' TSE-PSYCHEDELIC experiment that yields individual geminal ¹H-¹H couplings at pure shift resolution. This new experiment – a variation on the original TSE-PSYCHEDELIC^[5] – works well as long as the parent TSE-PSYCHE experiment^[7] is able to resolve the pure shift responses of both geminal protons. This allows straightforward extraction of two-bond *J*-coupling and RDC magnitudes in several cases that until now were considered challenging. The new method will be very useful for configurational and conformational analysis.

- 1. W.A. Thomas. Prog. Nucl. Magn. Reson. Spectrosc. 1997, 30, 183-207.
- 2. G. Kummerlöwe & L. Burkhard. TrAC Trends Anal. Chem. 2009 28, 483-93.
- 3. P. Tzvetkova, S. Simova & L. Burkhard. J. Magn. Reson. 2007 186, 193-200.
- 4. N. Marco, P. Nolis, R.R. Gil & T. Parella. J. Magn. Reson. 2017 282, 18-26.
- 5. D. Sinnaeve, J. Ilgen, M.E. Di Pietro, J.J. Primozic, V. Schmidts, C.M. Thiele, B. Luy. *Angew. Chem. Int. Ed.* 2020 **59**, 5316-20.
- 6. F.X. Cantrelle, E. Boll & D. Sinnaeve. Anal. Chem. 2024 96, 7056-64.
- 7. M. Foroozandeh, R. W. Adams, P. Kiraly, M. Nilsson, G. A. Morris. *Chem. Commun.* 2015 **51**, 15410-3.

Multi-harmonic EPR detection of melanin in skin melanomas: from mice to men

Mohammad Wehbi¹, Lionel Mignion², Nicolas Joudiou², Evelyne Harkemanne³, and Bernard Gallez^{1,2*}

Over the last decades, the incidence of melanoma has been continuously increasing. Today, melanoma remains the most aggressive skin cancer, significantly reducing survival rates for patients in its advanced stages. Therefore, early diagnosis remains the key to change the prognosis of patients with melanoma. Eumelanin, the main pigment present in melanomas, is paramagnetic and detectable by EPR. We previously described that images obtained using 9 GHz EPR imaging could be overlaid on histological images [1]. In parallel, ex-vivo measurements of human biopsies showed that the EPR signal in benign nevi was significantly lower than that in malignant melanomas and found a correlation between the EPR signal and Breslow depth (tumor thickness in the skin) [2]. This led us to succeed in detecting noninvasively the melanin signal from skin melanoma models in mice at low frequency EPR (1GHz) [3,4]. We performed a clinical study using a whole-body EPR system (ClinEPR), in patients on skin lesions suspicious of melanoma. EPR data obtained before surgery were compared with histopathology results. The EPR signal of melanin was significantly higher (p<0.0001) in melanoma lesions (n=26) than that in benign atypical nevi (n=62). A trend toward a higher signal intensity (though not significant) was observed in high Breslow depth melanomas (a marker of skin invasion) than in low Breslow lesions [5]. Because the melanin signal recorded was at the limit of the noise, there was a clear room for boosting the sensitivity of the method through improvement in instrumentation.

Our clinical EPR system has been very recently upgraded with the capability to apply larger modulation amplitude and to record/analyze the EPR signal in **multi-harmonics** mode (*Novilet*) [6]. We have compared the melanin signal obtained on phantoms using classical CW-EPR (1st harmonic) and multi-harmonics mode. We observed a boost in sensitivity by a factor about 10. In nude hairless mice (n=8) with implanted skin B16 melanomas, we observed a **boost in sensitivity** *in vivo* similar to that *in vitro* with the capability to detect melanoma cells in the skin at an earlier stage of development. Multi-harmonic EPR was also able to detect non-invasively a signal coming from melanoma cells in lymph nodes [8]. A new clinical study is presently ongoing to assess the capability of the technology to characterize noninvasively suspect pigmented lesions. An intermediate analysis of the first 99 lesions in patients shows that multi-harmonic EPR can differentiate melanoma significantly from benign nevi. We also aim to compare the EPR results to the diagnostic performance of dermoscopy and confocal microscopy applied on the same lesions.

- 1. Q. Godechal et al., Exp. Dermatol. (2012) 21, 341-346
- 2. E. Cesareo et al., PLoS One (2012) 7, e48849
- 3. E. Vanea et al., *NMR Biomed* (2008) 21, 296-300
- 4. C. Desmet et al., Free Rad Res (2019) 53, 405-410
- 5. L. Mignion, et al, Free Rad. Biol. Med. (2022) 190, 226-233
- 6. M. Gonet, et al., Free Radic Biol Med. (2020) 152, 271-279
- 7. M. Wehbi, et al., *Mol Imaging Biol.* (2024) 26, 484-494

¹Biomedical Magnetic Resonance Research Group, Louvain Drug Research Institute, Université catholique de Louvain (UCLouvain), Brussels, Belgium

²Nuclear and Electron Spin Technologies (NEST) platform, Louvain Drug Research Institute, Université catholique de Louvain (UCLouvain), Brussels, Belgium

³Department of Dermatology, Melanoma Clinic, King Albert II Institute, St Luc Hospital, Université catholique de Louvain (UCLouvain), Brussels, Belgium

Unravelling competitive adsorption in zeolites with solid-state NMR

S. Radhakrishnan^{1,2}, C. Vinod Chandran^{1,2}, A. Morais^{1,2}, G. Arbiv^{1,2,3}, J. A. Martens^{1,2}, E. Breynaert^{1,2,3*}

^{1.} NMR/X-ray Platform for for Convergence Research (NMRCoRe) & Centre for Surface Chemistry and Catalysis - Characterization and Application Team (COK-KAT), KU Leuven, Belgium ³ Center for Molecular Water Science (CMWS), Hamburg, Germany

Aluminosilicate zeolites are indispensable industrial catalysts whose performance depends on molecular adsorption inside their pores. Their performance is governed by molecular adsorption inside the pores, where host–guest interactions include Brønsted acid site interactions, hydrogen bonding, dispersion forces, etc. Adsorption locations depend strongly on the properties of the guest molecules as well as polarity differences within the crystal, making it crucial to understand these processes for tuning selectivity and preventing deactivation. Competitive adsorption between water and organics is particularly relevant to aqueous-phase catalysis, yet remains poorly understood at the molecular level.

Solid-state NMR provides unique quantitative and site-specific insights into these processes. Absolute quantitative NMR enables adsorption isotherms via in situ standard addition in the rotor, while lineshape and relaxation (T_1 , T_2 , $T_1\rho$) distinguish bulk and confined molecules and probe adsorbate—surface interactions. Homonuclear correlation (RFDR, EXSY, DQ–SQ), multinuclear through-bond (INEPT, HSQC, HMBC) and dipolar-based (CPMAS, CP-HETCOR) experiments further resolve host—guest interactions and competition. The observations from ssNMR in combination with complementary techniques such as X-ray diffraction, FTIR spectroscopy, modeling within a convergent research approach, in-depth material characterization, and selective pore blocking or active site poisoning experiments, allows detailed mapping of adsorption sites and mechanisms.

The following case studies will be presented: (i) Toluene–water adsorption: Toluene interacts mainly via dispersion and π interactions, while water strongly binds to Brønsted acid sites and silanols¹; (ii) Furfuryl alcohol polymerization in ZSM-5: Confocal microscopy and ssNMR showed that solvent polarity controls whether polymerization occurs in straight or sinusoidal channels²; (iii) In β -citronellene hydroalkoxylation over beta zeolites, competitive adsorption of alcohols and water can block zeolite pores, forcing β -citronellene to react at pore mouths, steering product selectivity.⁴

Together, these results demonstrate the power of solid-state NMR to map adsorption sites, quantify competitive adsorption, and uncover mechanisms inaccessible by other methods. They also emphasize the need for in situ, multi-diagnostic approaches to capture molecular arrangements and dynamics across time and length scales, enabling zeolite design tailored to application.

- 1. G. Arbiv, S. Radhakrishnan, A. F. Morais, C. Vinod Chandran, D. Vandenabeele, D. Dom, K. Duerinckx, C.E.A. Kirschhock and E. Breynaert, 2025, arXiv.2509.10219
- 2. S. Radhakrishnan, C. Lejaegere, K. Duerinckx, W.S. Lo, A.F. Morais, D. Dom, C.V. Chandran, I. Hermans, J.A. Martens, E. Breynaert, Mater Horiz 10 (2023) 3702–3711.
- 3. A. V. Kubarev, E. Breynaert, J. Van Loon, A. Layek, G. Fleury, S. Radhakrishnan, J. Martens, M.B.J. Roeffaers, ACS Catal 7 (2017) 4248–4252.
- 4. S. Radhakrishnan, P.J. Goossens, P.C.M.M. Magusin, S.P. Sree, C. Detavernier, E. Breynaert, C. Martineau, F. Taulelle, J.A. Martens, J Am Chem Soc 138 (2016) 2802–2808.

Mapping Cancer's Metabolic Footprint: Plasma NMR for Early NSCLC Diagnosis

J. Meynen¹; P. Adriaensens²; M. Criel^{1,3}; K. Vanhove^{1,4,5}; M. Thomeer³; L. Mesotten^{1,6}; E. Derveaux²

- 1 Faculty of Medicine and Life Sciences, Hasselt University, Hasselt
- 2 Analytical and Circular Chemistry, NMR Group, Institute for Materials Research (Imo-Imomec), Hasselt University, Diepenbeek
- 3 Department of Respiratory Medicine, Ziekenhuis Oost-Limburg, Genk
- 4 Department of Respiratory Medicine, University Hospital Leuven, Leuven
- 5 Department of Respiratory Medicine, Algemeen Ziekenhuis Vesalius, Tongeren
- 6 Department of Nuclear Medicine, Ziekenhuis Oost-Limburg, Genk

Despite the advancements in diagnostic imaging, surgical techniques, and targeted therapies, the overall prognosis for lung cancer patients remains poor. Consequently, lung cancer persists as the most prevalent form of cancer and the primary cause of cancer-related mortality on a global scale. The poor prognosis and high mortality rate are largely a consequence of delayed diagnosis, which is primarily attributed to the absence of symptoms in the early stages of the disease. This is also reflected by the disparity in five-year survival rates between patients with localized and distant lung cancer, which are approximately 67% and 12%, respectively. It is therefore imperative to diagnose the disease in an early stage, before the emergence of clinical symptoms, to enhance overall survival rates. Several screening techniques have been evaluated in high-risk patients, including low-dose computed tomography (LDCT). However, the use of LDCT is constrained by its high costs, the likelihood of overdiagnosis, and the occurrence of false-positive results. To address these limitations, the integration of **biomarkers**, either as standalones or in conjunction with existing screening techniques, holds promise for enhancing diagnostic accuracy in a non-invasive manner.

Biomarkers are defined as measurable biological molecules that can be found in body fluids or tissues and that indicate the presence or absence of a condition or disease. Metabolomics is an interesting domain for the identification of potential biomarkers as it reflects a real-time physiological state. As soon as lung cancer arises during early tumorigenesis, metabolic shifts can be determined through mass spectrometry (MS) or **proton nuclear magnetic resonance** (¹H-NMR). ¹H-NMR has several advantages over MS, including minimal and non-destructive sample preparation and high reproducibility.

This research, therefore, aims to identify potential plasma-based biomarkers for the early detection of the most common type of lung cancer, non-small cell lung cancer (NSCLC), using ¹H-NMR based metabolomics. To this end, a prospective, interventional longitudinal clinical study was conducted, encompassing patients diagnosed with resectable stage I-IIIA NSCLC. Plasma samples were collected at six different timepoints, including two preoperative (on the day of diagnosis, T1; and on the day of surgery, T2) and four postoperative timepoints (four weeks, T3; six weeks, T4; twelve weeks, T5; and one year after surgery, T6). The preoperative plasma samples can be considered as early-stage NSCLC samples, while the postoperative plasma samples can be considered as samples from healthy individuals, as patients who showed disease recurrence within 24 months after surgery were excluded from further analyses. All plasma samples were measured using a semi-targeted ¹H-NMR approach, resulting in 228 well-defined integration regions that represent the concentration of 62 different metabolites. These 228 integration regions were used as the variables for multivariate statistical analyses, including orthogonal partial least squares discriminant analysis (OPLS-DA) and OPLS-effect projections (OPLS-EP). The most differentiating variables, and therefore potential biomarkers, were identified using the variable importance for projection (VIP) analysis.

A comparison of the plasma metabolite profiles at the different timepoints using OPLS-DA reveals a clear distinction between the preoperative and postoperative samples, all with sensitivity, specificity, and accuracy values of at least 90%. A subsequent VIP analysis showed that lactate, asparagine, acetate, and cysteine were the primary contributors to the observed differentiation. This set of four metabolites, therefore, possesses the potential to serve as early-stage metabolic biomarkers for NSCLC.

Solution-state NMR spectroscopic characterization of metal-organic assemblies

R. Lavendomme^{1,2}

¹ Laboratoire de Résonance Magnétique Nucléaire Haute Résolution, Université libre de Bruxelles

Self-assembly of metal and organic ligands has become a powerful tool to generate a diversity of metal-organic assemblies with specific shape and functions such as metal-organic cages, helicates, knots, catenanes. It can be challenging to identify the structure of such assemblies and characterize their key properties for applications. In this communication we will delve into different aspects of discrete metal-organic assemblies that can be characterized via solution-state NMR spectroscopy: size and shape identification, isomerism, conformational dynamics, and host–guest properties (Figure 1).

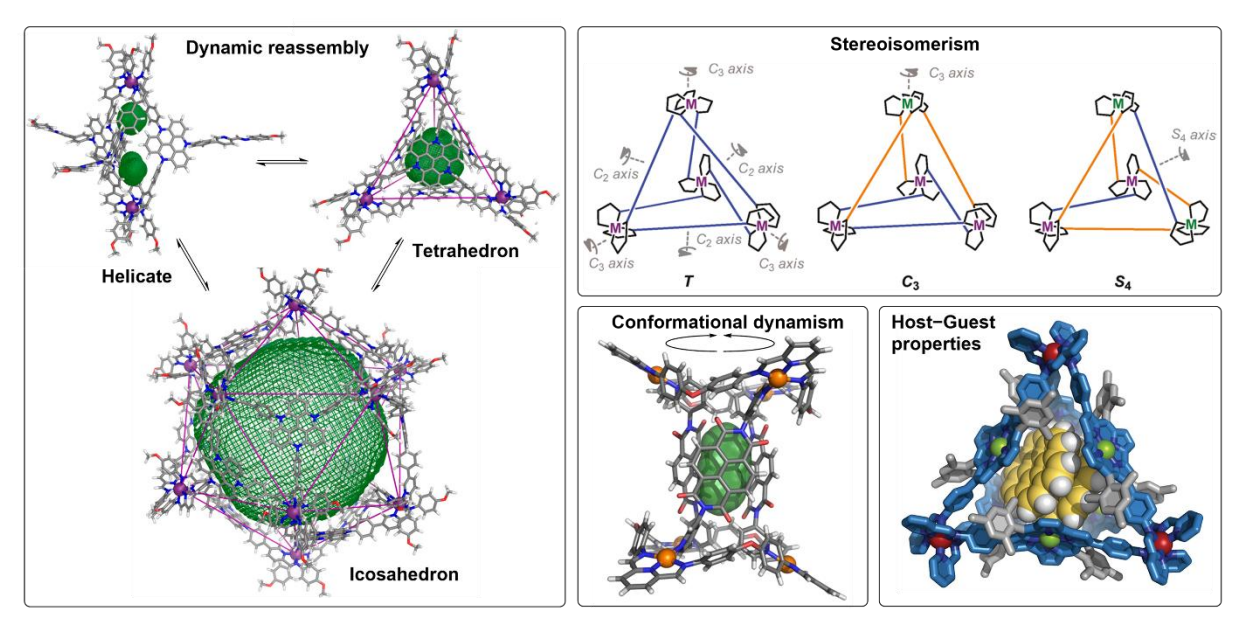


Figure 1. Selected aspects of metal-organic assemblies that can be characterized by solution-state NMR spectroscopy.

- 1. Lavendomme, R., Ronson, T. K., Nitschke, J. R. J. Am. Chem. Soc. 2019, 141, 12147–12158.
- Zhang, D., Gan, Q., Plajer, A. J., Lavendomme, R., Ronson, T. K., Lu, Z., Jensen, J. D., Laursen, B. W., Nitschke, J. R. J. Am. Chem. Soc. 2022, 144, 1106–1112.
- Meng, W, Clegg, J. K., Thoburn, J. D., Nitschke, J. R. J. Am. Chem. Soc. 2011, 133, 13652– 13660.
- 4. Xu, Y., Li, G., Liang, S., De Leener, G. Luhmer, M., Lavendomme, R., Gao, E.-Q., Zhang, D. *Angew. Chem. Int. Ed.* 2025, **64**, e202507981.
- 5. Carpenter, J. P., McTernan, C. T., Greenfield, J. L., Lavendomme, R., Ronson, T. K., Nitschke, J. R. *Chem* 2021, **7**, 1534–1543.
- 6. Yamashina, M., Tanaka, Y., Lavendomme, R., Ronson, T. K., Pittelkow, M., Nitschke, J. R. *Nature* 2019, **574**, 511–515.

² Laboratoire de Chimie Organique, Université libre de Bruxelles

ABSTRACTS POSTER CONTRIBUTIONS

List of Posters

- **P1**. Unravelling the Role of Structure and Defects in Reduced Commercial Titania with Potential for Visible-Light Photocatalysis
- L. Van den Bergh (Flash)
- **P2**. Assessing acid properties of heterogeneous acid nanosilica catalysts by solid-state NMR for biomass valorisation
- Z. Vanboucq
- **P3**. Quantitative multinuclear MAS NMR spectroscopy reveals why NH3 TPD severely underestimates dealumination of zeolites upon hydrothermal aging E. Breynaert (Flash)
- **P4**. Largest macrocyclic Pseudomonas CLiP Tanniamide: Structure, Dynamics, and effects of linearization
- D. Prasad
- **P5**. Examining cation dynamics in layered 2D hybrid organicinorganic perovskites using solid-state NMR
- E. Garip (Flash)
- **P6**. Unveiling the activity-acidity correlation via 31P-ssNMR of TMP: a study on metal(IV)-doped silica-based catalysts
- M.Saitta
- P7. Computational optimization of 3D-printed flexible MRI receive coils
- Q. Goudard (Flash)
- P8. Comparison of processing tools for metabolomics by NMR
- M. Kolkman
- **P9**. Toward reliable molar mass determination of glycolated polymer channel materials for organic electrochemical transistors
- L. Bynens (Flash)
- **P10**. Predictive Modeling of Phosphorus NMR Parameters in Intrinsic and Post-Synthetically Functionalized Porous Materials
- R. M. Narváez
- **P11**. A Quadruplex-Triplex Hybrid with a Pseudo Three-Layered Core of a Codeine Aptamer
- L.Y. M. Vianney (Flash)

- **P12**. Zirconium (IV) layered phosphonate-phosphate as catalysts for the valorization of glycerol
- N. Ghanemnia
- **P13**. Al-Driven Analysis of Multiparametric MRI for Evaluating Response to Targeted and Immune Therapies in Preclinical Melanoma Models Madeline El Assal (Flash)
- **P14**. Monte Carlo Simulations of the T₂ relaxivity induced by Exotic-Shaped Superparamagnetic Nanoparticles
- F. Fritsche
- **P15**. Insights into the crystallisation of simple organic salts using multinuclear NMR in the liquid state
- L. Fusaro (Flash)
- **P16**. Beware of the structure: Insights into the Phosphorus Dynamics of post-synthetically modified NU1000 in the presence of water
- J. Theissen
- **P17**. Structural Insights into Acyl Chain–Dependent Membrane Interactions of Pseudomonas Cyclic Lipodepsipeptides
 Xinyu Qian (Flash)

Please put up your posters in the board with your assigned number by lunch on Thursday

Remove your poster during the final coffee break in the afternoon on Friday

Unravelling the Role of Structure and Defects in Reduced Commercial Titania with Potential for Visible-Light Photocatalysis

L. Van den Bergh^{1,2}, S. Van Doorslaer², V. Meynen¹

Titanium-dioxide materials are known semiconductors with divers applications in chemical catalysis, the food industry and energy conversion. Several of these applications use the photocatalytic property of titania, which is mostly active in the UV part of the electromagnetic spectrum. By chemically reducing the normally white titania, it can acquire colour, which makes it active in also the visible part of the electromagnetic spectrum [1]. However, in literature there is a lot of contradiction on the most appropriate reduction process and its influence on the properties and photocatalytic activity of the coloured titania. In this project, titania is reduced using a thermal process with NaBH4 as reducing agent [2]. It appears that the reduction is sensitive to many different parameters of the process which are hard to monitor, such as the argon flow or temperature, leading to problems in reproducibility.

In a previous study, another key parameter of reduction, the crystal structure of phase pure titania materials, was investigated, where it was attempted to create a clear overview on the influence of the crystal structure of titania on the reduction [3]. However, it's the more commercially available materials that are of bigger interest to use as photocatalysts, as they are less expensive and more easily available, compared to the very phase pure nanomaterials with specific crystal size. For example, the well-known P25 is often used for its favourable catalytic properties, making it an interesting material to reduce with the intent to even further improve its photocatalytic activity [4]. In this study four commercially available titania materials were reduced and characterized with different spectroscopic techniques, such as EPR, XRD, in-situ drift-FT-IR and UV-Vis DR. EPR, as one of the key techniques reveals insight in the nature of the Ti(III) centres and other defects formed upon reduction of the titania. The effect of the change in crystal structure in the commercial materials is compared with the effect of the reduction on the phase pure samples. Additionally, the effect of other properties, such as crystal size and porosity, on the reduction and vice versa are discussed in this work.

- 1. T.S. Rajaraman et al., Chemical Engineering Journal 2020, 389.
- 2. D. Ariyanti et al., Materials Chemistry and Physics 2017, 199, 571-576.
- 3. L. Van den Bergh et al., Manuscript in preparation.
- 4. M.C. Thurnauer et al, Journal of Physical Chemistry 2003, 107, 4545-4549.

¹ LADCA, Department of Chemistry, University of Antwerp.

² TSM², Department of Chemistry, University of Antwerp.

Assessing acid properties of heterogeneous acid nano-silica catalysts by solid-state NMR for biomass valorisation

Z. Vanboucq ^{1,2}, M. Saitta ^{1,2}, A. Morena ¹, M. Ngueteu Tongnang ¹, L. Fusaro ¹, S. Hermans ², C. Aprile ¹

The depletion of petroleum resources and the rising energy demand provoked the need for sustainable alternatives such as biofuels. However, their production generates around 10% (w/w) glycerol as a by-product [1]. Valorising this compound fits within a circular economy approach. The acetalization of glycerol with acetone, catalysed by an acid, leads to the formation of solketal, a valuable fuel additive [2]. The conversion of glycerol into solketal requires a catalyst with Brønsted acidity [3].

To assess both the strength and the nature of acid sites in a solid catalyst (Brønsted or Lewis), trimethylphosphine (TMP) can be employed as a probe molecule in solid-state Nuclear Magnetic Resonance (NMR) investigations. TMP may either be protonated by a Brønsted site or coordinated to the lone pair of a Lewis site. These distinct interactions result in characteristic chemical shifts of the phosphorus signal in ³¹P NMR spectra ^[3,4]. Therefore, the use of probe molecules in solid-state NMR represents a valuable approach to assess the acidity of catalysts, thereby guiding the design of solid acids tailored for the glycerol-to-solketal conversion.

In this work, three morphologies of silica nanoparticles (hollow nanospheres, nanotubes and dendrites) were functionalised with a sulfonic acid, introducing strong Brønsted acid sites. Both the functionalisation degree and the nature of the sulfonic active sites were investigated using ²⁹Si and ¹³C solid-state NMR (*Figure 1*) and X-Ray Photoelectron Spectroscopy (XPS) respectively. The acidity was further assessed by ³¹P solid-state NMR using TMP. By probing acidity through solid-state NMR, we aim to establish a correlation between the acid properties and the catalytic reactivity, as the three heterogeneous catalysts were highly active in the conversion of glycerol to solketal.

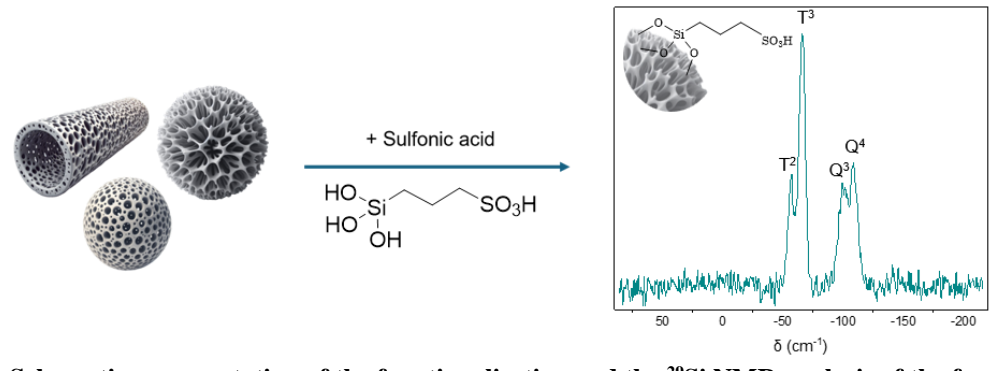


Figure 3: Schematic representation of the functionalisation and the ²⁹Si NMR analysis of the functionalised silica nanoparticles.

- [1] F. Yang, M. A. Hanna, R. Sun, Biotechnol Biofuels 2012, 5, DOI: 10.1186/1754-6834-5-13.
- [2] L. Li, T. I. Korányi, B. F. Sels, P. P. Pescarmona, *Green Chemistry* **2012**, *14*, 1611, DOI: 10.1039/c2gc16619d.
- [3] L. Soumoy, A. Morena, M. Armandi, S. Fiorilli, L. Fusaro, D. P. Debecker, C. Aprile, *J Catal* **2025**, 447, DOI: 10.1016/j.jcat.2025.116143.
- [4] A. Zheng, S. Bin Liu, F. Deng, *Chem Rev* **2017**, *117*, 12475, DOI: 10.1021/acs.chemrev.7b00289.

¹ Laboratory of Applied Materials Chemistry, UCNANO, Department of Chemistry, Namur Institute of Structured Matter (NISM), University of Namur, Namur 5000, Belgium

² Institute of Condensed Matter and Nanosciences (IMCN), Université catholique de Louvain (UCLouvain), Place Louis Pasteur, 1, Louvain-la-Neuve1348, Belgium

Quantitative multinuclear MAS NMR spectroscopy reveals why NH₃ TPD severely underestimates dealumination of zeolites upon hydrothermal aging.

S. Radhakrishnan¹, S. Singh^{2,3}, C. Vinod Chandran¹, H. Grönbeck³, T.V.W. Janssens² and <u>E.</u> Breynaert¹

¹.NMR/X-ray Platform for Convergence Research (NMRCoRe) & Centre for Surface Chemistry and Catalysis – Characterization & Application Team KU Leuven, Belgium. eric.breynaert@kuleuven.be.

The selective catalytic reduction of NOx by ammonia (NH₃-SCR) over Cu-zeolite catalysts, particularly Cu-chabazite (Cu-CHA), is a key technology for achieving near-zero NOx emissions in diesel and H₂ engines.[1] Under the harsh and dynamic conditions of exhaust systems, these catalysts deactivate due to degradation of the zeolite structure. The primary degradation pathway is dealumination, i.e., loss of framework aluminum atoms.[2] Dealumination proceeds via hydrolysis of Al–O–Si bonds when exposed to water vapor at high temperature, forming extra-framework Al species. Estimation of degree of dealumination and quantification of the resulting Al types, however, is not straightforward.

Temperature programmed desorption of ammonia (NH₃-TPD) is currently widely employed. Multinuclear solidstate NMR (1H, 27Al, and 29Si MAS NMR) experiments serve as a valuable tool to estimate the extent of dealumination (Figure 1), speciation of the dealumination products, their location and interactions: ²⁷Al NMR allows to identify quantitatively Al-species under different coordination states (4-, 5- or 6-coordinated); ²⁹Si NMR enables estimation of framework

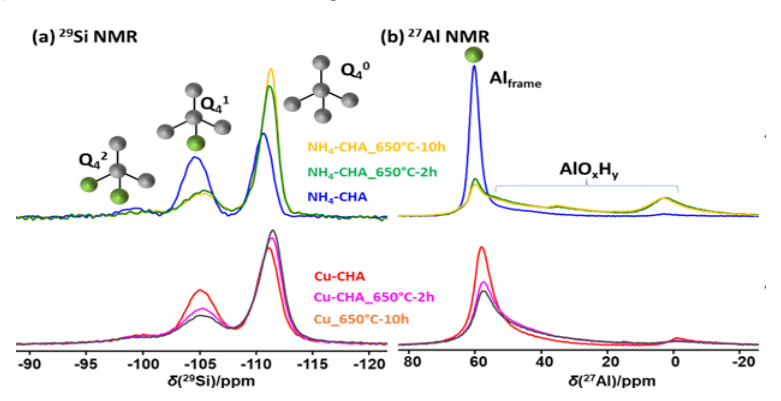


Figure 1. Comparison of the (a) 29 Si & (b) 27 Al direct-excitation NMR spectra for chabazite in NH₄+- (top) and Cu²⁺-exchanged (bottom) forms, hydrothermally aged at 650 °C for 2 or 10 hours, in 10% H₂O/10% O₂/N₂ atmosphere.

Al-content via the dependence of the chemical shift of a 29 Si site on its Al nearest neighbors (Q_n(xAl), n = t- & x = Al-neighbours; 1 H NMR allows to quantitatively determine different species – ammonium ions (NH₄+), Bronsted acid sites, aluminol (AlOH), silanol (SiOH), etc. During hydrothermal aging, extra-framework Al (5- and 6-coordinate), distorted tetrahedral Al, and new Q₄ 0 Si sites are formed (Figure 1), indicating both framework dealumination and partial framework healing. In Cu-exchanged zeolites, dealumination was significantly less severe than in the NH₄+ form. However, framework Al-content determined by 29 Si and 27 Al NMR far exceeded the Al-content determined by NH₃-TPD or NH₄+ quantified by 1 H NMR, suggesting additional charge balancing mechanisms. Together with 27 Al- 27 Al Double Quantum – Single Quantum NMR (DQ-SQ) a novel charge balancing mechanism - self-exchange of extraframework Al into ion-exchange sites was revealed. This mechanism leads to severe underestimation of framework Al content by NH₃-TPD. The finding has major implications for modeling zeolite dealumination, evaluating zeolite stability, and revisiting proposed Brønsted–Lewis acid site synergy mechanisms.

² Umicore Denmark ApS, Kogle Allé 1, 2970 Hørsholm, Denmark

^{3.} Department of Physics and Competence Centre for Catalysis, Chalmers University of Technology, SE412 96 Göteborg.

^[1] S. Radhakrishnan, S. Smet, C.V. Chandran, S.P. Sree, K. Duerinckx, G. Vanbutsele, J.A. Martens, E. Breynaert,

Temperature 1H NMR Spectroscopy, Molecules. 28 6456 (2023).

^[2] S. Singh, T.V.W. Janssens, H. Grönbeck, Catalysis Science & Technology Mechanism for Cu-enhanced hydrothermal stability of Cu – CHA for NH 3 -SCR, Catal. Sci. Technol. 14 3407(2024).

Largest macrocyclic *Pseudomonas* CLiP Tanniamide: Structure, Dynamics, and effects of linearization

<u>D. Prasad</u>¹, B. Kovács¹, P. Muangkaew³, N. Geudens¹, M. Hofte², A. Madder³ and J. C. Martins¹

¹NMR & Structure Analysis Unit, Dept. of Organic and Macromolecular Chemistry, Ghent University, Belgium ²Laboratory of Phytopathology, Department of Plants and Crops, Ghent University, Belgium. ³Organic Biomimetic Chemistry Research Group, Dept. of Organic and Macromolecular Chemistry Ghent University, Belgium

In the current era, as the world urgently transitions toward bio-based, sustainable alternatives in agriculture and faces the global threat of antimicrobial resistance (AMR), there is a critical need to explore novel candidates. Within this context, cyclic lipopeptides (CLiPs) a class of secondary metabolites produced by various strains of Pseudomonas, Bacillus, and Streptomyces have emerged as highly promising molecules, shaped by intense ecological pressures in the rhizosphere. This is exemplified by Bacillus-derived products used in commercial biocontrol agents and by daptomycin from Streptomyces. Compared with lipopeptides from Bacillus (three classes), Pseudomonas-derived CLiPs stand out for their remarkable chemical diversity, with more than 18 structurally recognized classes and over 130 unique CLiPs identified to date. Although Pseudomonas CLiPs have been extensively explored for their broad biological activities, including antifungal and antibacterial properties, far less is known about their structure-function relationships and biophysical mechanisms of action². Structural characterization remains a major bottleneck due to high chemical complexity and frequent stereochemical ambiguities. To study CLiPs in more detail, 3D structural models for particular classes are needed, alongside thorough structural investigations. Beyond static structures, understanding molecular dynamics is essential, as conformational flexibility often underlies biological activity. A clear example is daptomycin, where resistance is linked to hydrolysis of the depsipeptide bond. Similar hydrolytic processes have been observed in various Pseudomonas CLiPs in the context of bacterial defense and neutralization mechanisms in microbial warfare, yet the structural consequences of such linearization remain largely unexplored.3

In this study, we demonstrate an NMR-based stereochemistry dereplication approach, in combination with solid-phase peptide synthesis (SPPS) and biosynthetic gene cluster (BGC) analysis, for Tanniamide, a novel and the largest known macrocyclic CLiP in the *Pseudomonas* portfolio to date. NOE-based structure determination was carried out in a DPC micellar environment. Tanniamide was obtained in isotope-enriched form to probe its dynamics via Long range(LR) i to i+4 hydrogen bonds, and its backbone dynamics were investigated via ¹⁵N relaxation experiments. Water accessibility was probed via PRE titrations. Additionally, insights from LR-H bonds and PRE were complemented by MD simulation studies. We further investigated the effect of conformational dynamics of Tanniamide upon hydrolysis of the depsipeptide ester bond using ¹⁵N relaxation experiments. The studies showed that Tanniamide has a stable left handed helical conformation, which is lost upon hydrolysis, as indicated by the ¹⁵N relaxation data.

- 1 S. Götze and P. Stallforth, *Royal Society of Chemistry*, 2020, preprint, DOI: 10.1039/c9np00022d.
- N. Geudens and J. C. Martins, Front Microbiol, 2018, 9, 372540.
- 3 R. Hermenau, S. Kugel, A. J. Komor and C. Hertweck, 2020, preprint, DOI: 10.1073/pnas.2006109117.

Examining cation dynamics in layered 2D hybrid organic-inorganic perovskites using solid-state NMR.

E. Garip^{1,2}, P. La Magna³, E. Derveaux⁴, K. Van Hecke³, P. Adriaensens⁴, L. Lutsen^{1,2,5}, W. Van Gompel^{1,2,5}

Two-dimensional (2D) hybrid organic-inorganic perovskites are gaining increased research interest due to their potential applications in optoelectronic devices such as light-emitting diodes (LEDs) [1], photodetectors [2], and solar cells [3]. Their structure is composed of alternating layers of corner-sharing Pbl $_6$ octahedra, and organic spacer cations. Compared to their three-dimensional (3D) counterparts, 2D perovskites exhibit enhanced environmental stability [4,5]. In addition, since the organic cations are no longer confined within an octahedral cavity, they are not subject to the same size restrictions. This opens up a broad design space for incorporating diverse organic cations, enabling greater compositional and structural flexibility [6].

In this work, we investigate the structural and dynamic behavior of several 2D perovskites. Crystal structures are determined from single-crystal X-ray diffraction (SC-XRD) measurements, which reveal the presence of various non-covalent interactions between the cations. These interactions contribute to the rigidity of the organic layer, whereby more interactions usually give rise to a more rigid organic bilayer. To probe cation dynamics, we employ solid-state nuclear magnetic resonance spectroscopy (SS-NMR), analyzing both 13 C spectra and 13 C spin-lattice relaxation times (T_1). It is initially expected that 2D perovskites with a more rigid organic bilayer will exhibit the lowest cation mobility due to increased intermolecular interactions. However, our findings reveal that, although this expectation holds for some 2D perovskites, certain systems display higher cation mobility than those with fewer intermolecular interactions, as indicated by their lower T_1 values. This unexpected behavior suggests the presence of additional molecular motions that contribute to the observed reduction in T_1 .

- [1] Fakharuddin, A. et al., *Nature Electronics 2022*, 5(4), 203–216.
- [2] Han, J. et al., Nature Reviews Methods Primers 2025, 5(1).
- [3] Ollearo, R., et al., Science Advances 2023, 9(7).
- [4] Herckens, R. et al., Journal of Materials Chemistry A 2018, 6(45), 22899–22908.
- [5] Denis, P., et al., Advanced Optical Materials 2022, 10(18).
- [6] Van Gompel, W. T. M. et al., Journal of Materials Chemistry C 2023, 11(38), 12877–12893.

¹Hasselt University, Institute for Materials Research (imo-imomec), Hybrid Materials Design (HyMaD), Hasselt.

²Energyville, imo-imomec, Genk.

³Ghent University, Department of Chemistry, XStruct, Ghent.

⁴Hasselt University, Institute for Materials Research (imo-imomec), Applied and Analytical Chemistry, NMR group, Hasselt.

⁵imec, imo-imomec, Diepenbeek.

Unveiling the activity-acidity correlation via ³¹P-ssNMR of TMP: a study on metal(IV)-doped silica-based catalysts

M. Saitta ^{1,2}, A. Morena¹, M. Ngueteu Tongnang¹, A. Maertens ¹, L. Soumoy¹, L. Fusaro¹, S. Hermans², C. Aprile¹

The valorization of wastes is aligned with the need of finding new pathways to produce energy and useful chemicals, driven by the dream of a circular economy. In this context, the valorization of glycerol, the most abundant byproduct of the synthesis of biodiesel, gained the attention of academia and industry. From glycerol, it is possible to obtain solketal, a valuable chemical, via a ketalization reaction employing acetone. Another hot topic in this direction is the valorization of ligninocellulosic biomass, the most abundant biomass in the world. From it, it is possible to synthesize levulinic esters (like ethyl levulinate), which can be converted into y-valerolactone (GVL), a promising molecule usable as precursor for polymers or green solvent. The processes mentioned here are both acidcatalyzed reactions, requiring catalysts displaying different ratios of Lewis (L) and Brønsted (B) acidity to proceed (Figure 1).

The aim of this work was to understand the activity-acidity correlation of a series of catalysts, namely metal(IV)-doped silica-based materials, employing a solid state nuclear magnetic resonance (ss-NMR) approach. The solids, namely hollow silica nanospheres and nanotubes, were synthesized via a sol-gel route³ and characterized employing several techniques. The materials embedded different metal cations ($M = Ti^{4+}$, Zr^{4+} , Hf^{4+}), added to obtain different Si/M ratios in the final solids. To unveil how these parameters influenced the acidity of the catalysts, the strength and the L/B ratios of the acidic sites was explored performing ³¹P-ssNMR analysis of trimethyl phosphine (TMP), used as basic probe molecule.

Catalytic tests for the conversion of glycerol to solketal and for the conversion of ethyl levulinate to GVL were carried out employing the overmentioned heterogeneous catalysts. The catalytic activity of the solids was correlated to their acidic properties. It was found out that the higher the L/B ratio and the stronger the Lewis acid sites, the better the performances towards the synthesis of GVL, while the lower the L/B, the better the activity for the synthesis of solketal.

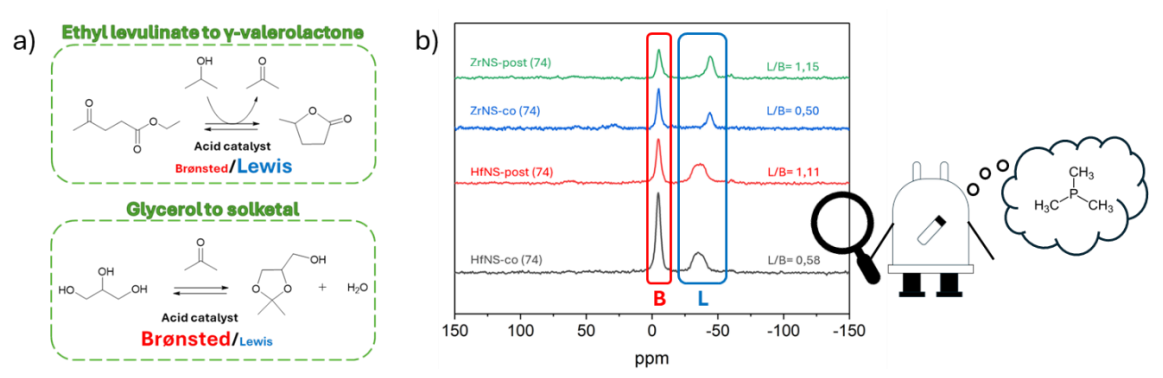


Figure 1. a) The two reactions studied; b) ³¹P-ssNMR spectra of TMP adsorbed on a series of acid nanosphere silica samples.

- 1. L. Wang, X. Du, D. Zhang, T. Hu, D. Ren. Chem. Select 2024, 9, e202400111.
- 2. M. Khalid, M. Granollers Mesa, D. Scapens, A. Osatiashtiani. *ACS Sustanaible Chem. Eng.* 2024, **12**, 16494-16517.
- 3. L. Soumoy, L. Fusaro, D. P. Debecker, C. Aprile, Chemistry of Materials 2023, 35, 1877-1890.

¹Laboratory of Applied Materials Chemistry, UCNANO, Department of Chemistry, Namur Institute of Structured Matter (NISM), University of Namur

² Institute of Condensed Matter and Nanosciences (IMCN), MOST division, Université catholique de Louvain

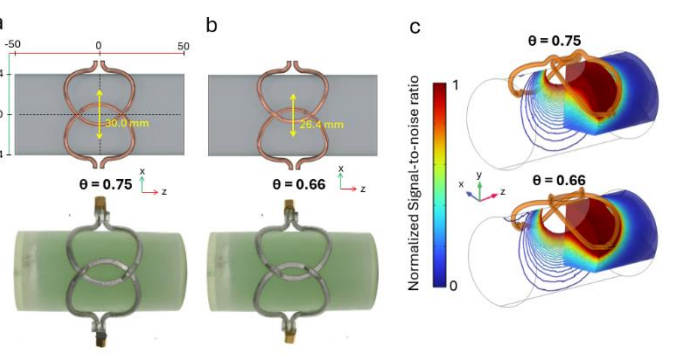
Computational optimization of 3D-printed flexible MRI receive coils

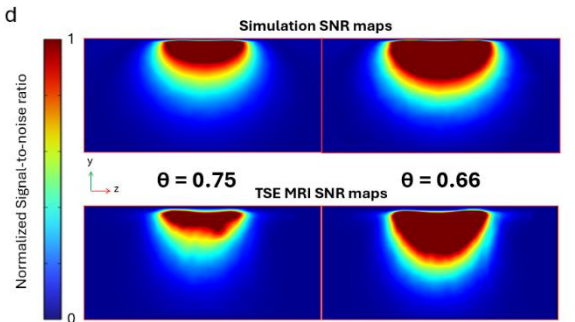
Q. Goudard^{1,2}, H. Vanduffel¹, C. Para-Cabrera¹, A. Vanduffel¹, D. Sakellariou¹, U. Himmelreich³, W. Vanduffel², R. Ameloot¹.

Introduction: Magnetic Resonance Imaging (MRI) is a widely used non-invasive technique in both clinical and research settings. Its effectiveness in demanding applications, such as functional MRI in animal models is often limited by low signal-to-noise ratio (SNR). The design of radiofrequency receive phased array coils remains largely manual, and is constrained by fabrication complexity and poor anatomical conformity. While custom-built hardware offers potential improvements,[1] traditional methods struggle to accommodate subject-specific constraints that can be mitigated using novel manufacturing techniques such as 3D-printing,[2] To address these challenges, we present a surface-

aware, parameterized modeling workflow thata digitally optimizes the geometry of a two-channel array coil at 3T. Using Finite Element²⁴ Method (FEM) simulations, the method iteratively adjusts the inter-coil distance to minimize coupling (S₂₁ parameter) thereby improving the SNR. The studied design is a two-channel surface array coil composed of overlapping 40 mm loops conformally placed on a cylindrical phantom (100 mm length, 48 mm diameter).

Method: The coil geometry was parameterized by the ratio of the center-to-center distance between coils to their diameter (θ). A surrogate gradient-descent algorithm integrating MATLAB, Python, and COMSOL Multiphysics was used to minimize S₂₁ and evaluate SNR across θ variations. Simulated SNR and SNR maps were computed using B_1^- and a noise correlation matrix derived from electric field distributions. Coils were fabricated via stereolithography





3D-printing (Form 3BL, Formlabs) using Flexible 80A resin, forming hollow channels later filled with conductive liquid metal (GalnSn alloy). The phantom was printed in Clear V4 resin and filled with a gel composed of water, agar, benzisothiazolinone, and copper(II) sulfate. MRI experiments were conducted on a 3T MAGNETOM Prisma scanner (AS82 CPL gradient coil, 80 mT/m, 200 T/m/s) using a Turbo Spin Echo sequence at 1 mm³ isotropic resolution. Experimental SNR maps were calculated in Python using SciPy and NumPy by convolving a 3×3 kernel to estimate local noise from segmented image regions.

Results: A state-of-the-art design (θ = 0.75) and an optimized design (θ = 0.66) were successfully printed (Figure 2a). The algorithm converged in 20 iterations. Specifically the system improved from an initial state (θ = 0.75) of S₂₁ = -4.82 dB and SNR = 1.37 x 10⁻⁵ to a better performance (θ = 0.66) with S₂₁ = -18.8 dB and SNR = 1.75 x 10⁻⁵, showing an increase of 27.7% of the simulated. Measurements at the 3T scanner shows a 25.3% improvement of the SNR for the same configuration.

- [1] T. Janssens *et al.*, « An implanted 8-channel array coil for high-resolution macaque MRI at 3T », *NeuroImage*, vol. 62, n° 3, p. 1529-1536, sept. 2012
- [2] H. Vanduffel *et al.*, « Additive Manufacturing of Subject-Conformal Receive Coils for Magnetic Resonance Imaging », *Adv Materials Technologies*, vol. 7, nº 12, p. 2200647, déc. 2022

¹ Center for Membrane Separations, Adsorption, Catalysis and Spectroscopy, KU Leuven

² Laboratory for Neuro- and Psychophysiology, Department of Neurosciences, KU Leuven

³ Biomedical MRI, Department of Imaging and Pathology, KU Leuven

YBMRS 25 – November 2025 – Floréal Blankenberge

Comparison of processing tools for metabolomics by NMR

M. Kolkman¹, P. De Tullio² & C. Damblon¹

Metabolomics approaches consist in the identification and quantification of metabolites (small molecules <1.5 kDa) in biofluids. Qualitative and quantitative analyses of these metabolites provide insights into the biochemical mechanisms underneath biological responses to perturbations and can support the discovery of biomarkers.

Biofluids are challenging matrices containing hundreds of metabolites at concentrations ranging from μM to mM in water. NMR spectroscopy is a convenient analytical method to analyse such samples, and stands out for its high reproducibility, non-destructive nature, non-specificity, robustness and quantification.^{1,2}

While data-acquisition presents a certain level of protocol standardisation, notably with the wide use of ¹H 1D experiment including solvent suppression, data-processing still lacks standardised procedures, with laboratories developing in-house software and protocols.³

In this work, we attempt a holistic comparison of various available processing software. The evaluation focuses on accuracy, precision, processing time, user-friendliness and cost. Furthermore, we investigate how each software addresses common challenges in metabolomics⁴, such as overlapping signals and low concentrations metabolites, and assess their suitability for the specific demands of metabolomics studies.

- 1. Giraudeau, P. Analyst. 2020, **145**, 2457-2472
- 2. Nagana Gowda, G. A. and Raftery, D. Analytical Chemistry. 2023, 95, 83-99
- 3. Andersson, E. R., et al. Anal. Chem. 2025, Article ASAP (DOI: 10.1021/acs.analchem.5c03274)
- 4. Dumez, J. N. Chemical Communications. 2022, **58**, 13855-13872

¹ Chimie Biologique Structurale, Université de Liège

²Center for Interdisciplinary Research on Medicines, Université de Liège

Toward reliable molar mass determination of glycolated polymer channel materials for organic electrochemical transistors

<u>Lize Bynens</u>¹, Jochen Vanderspikken¹, Daan Coenen¹, Sander Smeets¹, Peter Adriaensens¹, Koen Vandewal¹, Elien Derveaux¹, Wouter Maes¹

¹Institute for Materials Research (IMO), Hasselt University, Agoralaan 1, 3590 Diepenbeek, Belgium - Imec, Associated Laboratory IMOMEC, Wetenschapspark 1, 3590 Diepenbeek, Belgium

The molar mass of polymer channel materials plays a crucial role in the performance of organic electrochemical transistors (OECTs), significantly impacting their charge transport properties. While high-molar-mass polymers typically show an enhanced mobility (μ) and overall performance (μ C*), accurate molar mass determination remains very challenging, especially for glycolated polymers as used most often in OECTs. As a result, reported molar masses often lack validation, and literature comparisons become unreliable.

To address these challenges, dedicated batches of the benchmark p-type OECT material, pgBTTT, were synthesized using droplet flow chemistry, allowing control over molar mass via the residence time in the flow reactor. Preliminary OECT measurements suggest an optimal performance window at intermediate residence times. To accurately determine the molar mass, we are developing a new diffusion NMR calibration curve based on structurally matched gBTTT monomer, dimer, trimer, and two STM (scanning tunneling microscopy) characterized pgBTTT polymers. This approach aims to establish a reproducible link between synthesis conditions and device performance for glycolated materials.

Acknowledgement

This work was supported by Hasselt University and FWO Vlaanderen via the Hercules projects AUHL/15/2 - GOH3816N and I001324N and Ph.D. project 1S70122N.

References

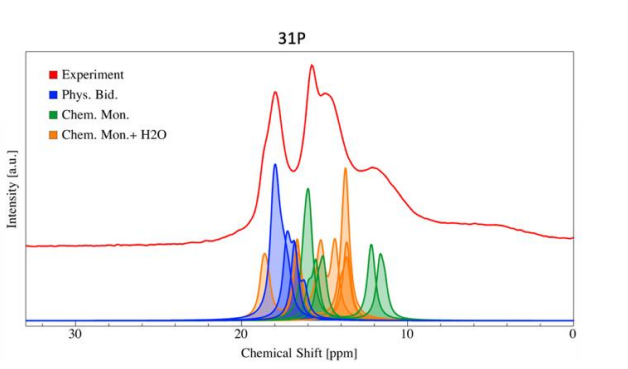
1. J. Tropp, et al. ACS Mater. Lett. 5 (2023), 1367-1375

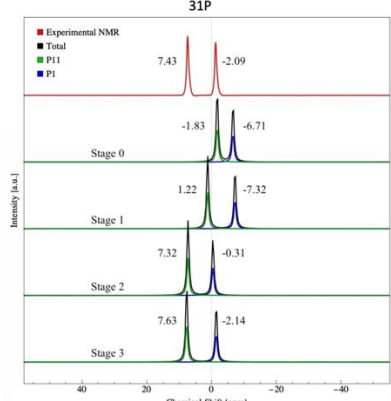
Predictive Modeling of Phosphorus NMR Parameters in Intrinsic and Post-Synthetically Functionalized Porous Materials

R. M. Narváez¹, J. Theissen^{3,4}, N. Gys^{1,3}, E. Derveaux⁴, P. Adriaensens⁴, W. Marchal⁴, R. Ameloot³, I. Tranca², T. Hauffman¹, and F. Tielens²

Porous materials constitute a versatile class of functional materials, defined by their tunable pore architectures, high surface areas, and diverse chemical environments that enable applications ranging from catalysis and gas storage to drug delivery and energy conversion. Within this broad family, porous materials that either inherently contain phosphorus in their structure (Al-CAU-67) or are functionalized with phosphorus species represent a distinctive subclass, as phosphorus imparts unique electronic, coordination, and acid base characteristics. However, their structural complexity poses significant challenges for experimental characterization. Traditional techniques such as X-ray diffraction and solid-state NMR often struggle to provide unambiguous information on the local phosphorus environment, pore connectivity, and atomic-level arrangement. To overcome these limitations, density functional theory (DFT) calculations, including GIPAW methodologies, are combined with advanced spectroscopic techniques, allowing complementary insights into the structural arrangements and properties of these systems, as well as direct comparison with experimental NMR data.

In this study, we present two illustrative examples of phosphorus in porous materials. The first example focuses on AI-CAU-67, a porous framework that intrinsically contains phosphorus, allowing us to evaluate the effects of ab initio structural relaxation on the ³¹P NMR spectra, as well as the quadrupolar coupling observed in the ²⁷AI NMR spectrum. The second example focuses on the NU-1000 structure, a MOF constructed from Zr₆ clusters and pyrene-based TBAPy⁴⁻ linkers, featuring hierarchical pore system with two distinct cavity sizes. Here, phosphonate functionalization with Phenylphosphonic acid enables the study of adsorption behaviour and the influence of water molecules within the NU-1000 framework. Together, these examples demonstrate that combining computational modelling with NMR spectroscopy provides detailed insight into both native and functionalized phosphorus environments in porous materials.





References

1. Theissen, Jennifer, et al. "Isoreticular Expansion in Porous Al (III) and Ga (III) Phosphonates: Synthesis, Structure, and Properties." (2025).

¹ Electrochemical and Surface Engineering (SURF) Research Group, Vrije Universiteit Brussel.

² General Chemistry (ALGC) Materials Modelling Research Group, Vrije Universiteit Brussel.

³ Center for Membrane Separation, Adsorption, Catalysis and Spectroscopy (cMACS), KULeuven.

⁴ Analytical and Circular Chemistry (ACC), Institute for Materials Research (IMO), Hasselt University.

A Quadruplex-Triplex Hybrid with a Pseudo Three-Layered Core of a Codeine Aptamer

Y. M. Vianney, J. C. Martins

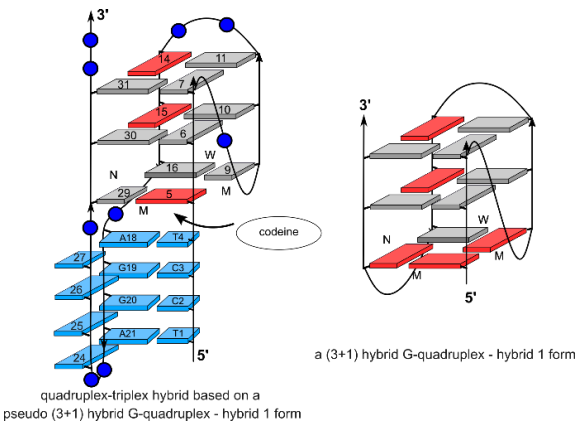
NMR and Structure Analysis Unit, Department of Organic and Macromolecular Chemistry, Ghent University, Ghent

DNA can adopt a wide array of three-dimensional structures beyond the canonical B-form. One way to exploit this structural diversity for technological application is through the use of aptamers. These are DNA-based single-stranded nucleic acids that exhibit high affinity and selectivity towards specific target molecules, ranging from ions and small molecules to proteins and even whole cells. Despite the large number of reported aptamer sequences, very few have advanced beyond proof-of-concept studies. A major obstacle in this respect is the limited structural understanding of aptamers.

Among non-canonical structures, G-quadruplexes, secondary structures formed by guanine (G)-rich sequences, have been observed in some aptamer structures. Recently, more complex tertiary fold architectures have been reported, such as the quadruplex-duplex hybrids. A candidate aptamer of particular interest is the **codeine-binding aptamer**, which has been proposed to contain a G-quadruplex element. However, the sequence proposed in the original work is prone to aggregation, complicating its structural characterization.

Using the principles driving G-quadruplex folding geometry and guided by NMR data, we redesigned the codeine aptamer sequence to favor a predominant fold capable of binding codeine. Spectral assignment revealed that the codeine aptamer adopts a three-layered tetrad core embedded in a quadruplex-triplex (QT) hybrid structure. Preliminary analysis of the codeine-DNA NOE contacts locates the codeine at the quadruplex-triplex interface.

The glycosidic torsion angle pattern (*syn-anti* pattern) and thus the folding resemble those of a (3+1) hybrid topology categorized as the hybrid 1-type with a propeller, lateral, lateral (-pll) loop progression. However, unlike typical G-quadruplexes, the tetrad core is composed of two G-tetrads (upper and middle) and one GCGC tetrad at the bottom. The structure adopted by this codeine aptamer challenges and expands the current framework of G-quadruplex folding and classification.



- 1. Lim, K. W., & Phan, A. T. (2013). Angew. Chem. Int. Ed., 52, 8566-8569.
- 2. Vianney, Y. M., & Weisz, K. (2022). Nucleic Acids Res., 50, 11948-11964.
- 3. Bing, T., Zheng, W., Zhang, X., Shen, L., Liu, X., Wang, F., ... & Shangguan, D. (2017). *Sci. Rep.*, *7*, 15467.

Zirconium (IV) layered phosphonate-phosphate as catalysts for the valorization of glycerol

Nahal Ghanemnia^{1,+}, Martina Saitta^{2,3,+}, Elien Derveaux^{1,4}, Richa Tomer^{3,6}

Nick Gys^{5,6}, Peter Adriaensens^{1,4}, Sophie Hermans^{*,3} Carmela Aprile^{*,3} Wouter Marchal^{*,1}

- ¹ Analytical and Circular Chemistry, Institute for Materials Research (imo-imomec), Hasselt University, Agoralaan Gebouw D, 3590 Diepenbeek, Belgium
- ² Laboratory of Applied Materials Chemistry, UCNANO, Department of Chemistry, Namur Institute of Structured Matter (NISM), University of Namur, 5000 Namur, Belgium
- ³ Université catholique de Louvain (UCLouvain), Institute of Condensed Matter and Nanosciences (IMCN), Place Louis Pasteur, 1, 1348 Louvain-la-Neuve, Belgium
- ⁴ Analytical and Circular Chemistry, NMR Group, Hasselt University, Campus Diepenbeek Gebouw D, 3590 Diepenbeek, Belgium
- ⁵ Sustainable Materials Engineering (SUME), Research Group of Electrochemical and Surface Engineering (SURF)Vrije Universiteit Brussel, Pleinlaan 2, 1050, Brussels, Belgium
- ⁶ Centre for Membrane Separations, Adsorption, Catalysis, and Spectroscopy (cMACS), KU Leuven, Celestijnenlaan 200F, 3001 Leuven, Belgium

The acetalization of crude glycerol with acetone to form solketal is a promising valorization pathway for this major biodiesel byproduct ¹, provided that efficient and stable acid catalysts are available. In this work, hybrid porous zirconium phosphonate—phosphate materials² were synthesized and investigated as recyclable heterogeneous catalysts. Their structure and acidity were elucidated primarily through solid-state NMR spectroscopy. ¹H-MAS-NMR and ³¹P-MAS- NMR both provided detailed insight into the environments of phosphate and phosphonate groups within the hybrid framework, while 2D-¹H-³¹P correlation experiments further revealed the connectivity between protons and phosphorus species. Together, these measurements enabled the identification of distinct acid sites and their roles in catalysis. The NMR findings were supported by ammonia TPD and XPS, confirming that phosphate incorporation enhances Brønsted acidity, stability, and recyclability. Under optimized conditions, the catalysts achieved solketal yields of up to 85% with 98% selectivity, and showed promising activity even at room temperature. This study highlights the central role of multinuclear and multidimensional solid-state NMR in the structural and acidity characterization of hybrid catalysts for biomass valorization.

- 1. Hoogendoorn, A. & van Kasteren, H. J. Enzymatic Biodiesel. *Transp. Biofuels* 131–180 (2010) doi:10.1039/9781849732277-00131.
- 2. Silbernagel, R., Martin, C. H. & Clearfield, A. Zirconium(IV) Phosphonate-Phosphates as Efficient Ion-Exchange Materials. *Inorg. Chem.* **55**, 1651–1656 (2016).

AI-Driven Analysis of Multiparametric MRI for Evaluating Response to Targeted and Immune Therapies in Preclinical Melanoma Models

Madeline El Assal 1, Lionel Mignion 2, Nicolas Joudiou 2, and Bénédicte F Jordan 1,2

- 1 Biomedical Magnetic Resonance Research Group (REMA), Louvain Drug Research Institute, UCLouvain (Université Catholique de Louvain), Brussels, Belgium
- Nuclear and Electron Spin Technologies Platform (NEST), Louvain Drug Research Institute, UCLouvain (Université Catholique de Louvain), Brussels, Belgium

Therapeutic resistance in advanced melanoma represents a critical barrier to durable clinical responses and is largely driven by dynamic intra-tumoral heterogeneity, which arises from both genetic and nongenetic mechanisms, including cellular plasticity and adaptive phenotypic reprogramming (1). (2) (3) (4) (5). Conventional imaging criteria, including RECIST, often fail to detect early or subtle changes in tumor biology, highlighting the need for predictive, non-invasive biomarkers capable of capturing dynamic alterations within the tumor microenvironment (6). The DREAM-MEL (Deep Radiomic Evaluation of AI-driven MRI in Melanoma) project seeks to address this challenge through the integration of multiparametric magnetic resonance imaging (mpMRI) with advanced deep radiomic analytics to quantitatively characterize tumor heterogeneity and predict therapeutic response.

In this study, longitudinal mpMRI acquisitions are performed in syngeneic murine melanoma models, incorporating diffusion-weighted ¹H MRI to assess cellular density and tissue microstructure, oxygenation-sensitive MRI (T₁ and T₂* mapping) to assess both tissue and vascular oxygenation, and localized PRESS spectroscopy to evaluate metabolic profiles (7). Together, these complementary imaging modalities enable high-dimensional phenotypic characterization of tumors, capturing both spatial and temporal heterogeneity at baseline and across multiple post-treatment time points following administration of BRAF/MEK-targeted therapy or anti-PD-1 immunotherapy.

High-dimensional radiomic features are extracted from the multiparametric datasets and integrated into a fully automated deep learning framework. Tumor segmentation is achieved using ensembles of 3D U-Net convolutional neural networks, providing precise delineation of regions of interest while excluding irrelevant anatomical structures (8). Segmented ROIs, together with oxygenation-sensitive and metabolic parametric maps, are processed through a decision network comprising eight modified ResNet-18 architectures adapted for multi-slice volumetric inputs (9). Feature representations are fused via convolutional and fully connected layers to generate predictive classifications of responder, partial responder, or non-responder phenotypes. Model training incorporates rigorous strategies, including data augmentation, batch normalization, dropout, and adaptive learning rate schedules, to ensure robust generalization and prevent overfitting, while dataset partitioning into training, validation, and testing subsets allows unbiased performance assessment (10) (11).

Experimental validation is performed in standardized murine melanoma models, including YUMMER 1.7 and YUMM 1.7 BRAF V600E variants, with longitudinal imaging correlated to tumor growth kinetics, survival outcomes, and ex vivo molecular analyses, including proliferation, apoptosis, hypoxia, and immune infiltration (3). Pilot studies optimized diffusion tensor imaging and PRESS acquisition protocols, confirming reproducibility, high spatial resolution, and sensitivity to key tumor microenvironment features.

The DREAM-MEL framework represents a novel paradigm for non-invasive, multiparametric phenotyping of melanoma, leveraging synergistic anatomical, metabolic, and oxygenation-sensitive imaging with deep radiomic analytics. By providing early, predictive biomarkers of therapeutic response, this approach supports precision oncology, facilitates personalized treatment strategies, and may ultimately improve patient outcomes by enabling timely adaptation of therapy based on tumor-specific heterogeneity.

Monte Carlo Simulations of the T₂ relaxivity induced by Exotic-Shaped Superparamagnetic Nanoparticles

F.Fritsche¹, G. Rosolen², A. De Corte², B. Maes², Y. Gossuin¹ and Q.L. Vuong¹

Nanoscale materials have garnered immense scientific interest over the past few decades due to their wide range of applications [1] and their unique properties, such as enhanced surface reactivity and quantum effects. Among them, SuperParamagnetic Iron Oxide Nanoparticles, typically composed of magnetite and maghemite, exhibit superparamagnetic behaviour at room temperature and possess a high surface area-to-volume ratio. These properties make SPIONs particularly valuable as T_2 or T_2^* contrast agents in Magnetic Resonance Imaging (MRI) for tumour detection. By reducing the transverse relaxation time (T_2) within targeted tumour tissues, SPIONs enhance image contrast between healthy and diseased regions, thereby improving diagnostic accuracy.

In this work, we investigate how the shape of SPIONs influences transverse relaxation T_2 . Relaxation was modelled by Monte Carlo simulations of CPMG sequences using nanoparticles ranging from 10 to 600 nm in diameter [2, 3]. The relaxivities $(1/T_2)$ of anisotropic shapes (cubes, cylinders and tetrahedra) were compared, volume-wise, with those of spheres. Furthermore, we propose a methodology [3] to predict the impact of arbitrary shapes on relaxation time based on Monte Carlo analysis of their magnetic stray field.

Contrary to prior experimental reports [4], our results indicate that relaxivity $(1/T_2)$ is not significantly impacted by particle shape. Only nanoparticles smaller than 30nm, in the motional average regime, show measurable differences, with some shapes exhibiting up to a 15% increase and others up to a 30% decrease.

- 1. Ito, A.; Shinkai, M.; Honda, H.; Kobayashi, T. "Medical Application of Functionalized Magnetic Nanoparticles". *Journal of Bioscience and Bioengineering*, 2005, 100, 1–11. https://doi.org/10.1263/jbb.100.1.
- Vuong, Q. L.; Gillis, P.; Gossuin, Y. "Monte Carlo Simulation and Theory of Proton NMR Transverse Relaxation Induced by Aggregation of Magnetic Particles Used as MRI Contrast Agents". *Journal of Magnetic Resonance*, 2011, 212, 139–148. https://doi.org/10.1016/j.jmr.2011.06.024.
- 3. Fritsche, F.; Rosolen, G.; De Corte, A.; Maes, B.; Gossuin, Y.; Vuong, Q.L. "Are nanocubes more efficient than nanospheres to enhance the nuclear magnetic relaxation of water protons? A Monte Carlo simulation study". *The journal of Chemical Physics*, 2025, 162(12). https://doi.org/10.1063/5.0251512
- 4. Andrade, R. G. D.; Veloso, S. R. S.; Castanheira, E. M. S. "Shape Anisotropic Iron Oxide-Based Magnetic Nanoparticles: Synthesis and Biomedical Applications". *International Journal of Molecular Sciences*, 2020, 21, 2455. https://doi.org/10.3390/ijms21072455.

¹ Biomedical Physics Unit, UMONS, Belgium.

² micro- and nano- Photonic Physics Unit, UMONS, Belgium.

Insights into the crystallisation of simple organic salts using multinuclear NMR in the liquid state

L. Fusaroa, V. Marsalaa, N. Tumanova, S. Colesb, P. Hortonb, G. Saiellic, R. Montisd

- ^a Namur Institute of Structured Matter, University of Namur, 5000 Namur, Belgium
- ^b School of Chemistry, University of Southampton, Southampton, UK
- ^c CNR Institute on Membrane Technology Unit of Padova, Via Marzolo, 1 35131 Padova, Italy
- d Università degli Studi di Urbino Carlo Bo, Via della Stazione 4, I-61029 Urbino, Italy

Small organic molecules typically form simple supramolecular assemblies, resulting in crystal structures with relatively small unit cells. However, we have recently isolated four novel crystalline phases (1–4) of fampridine hydrochloride (4-APH+Cl⁻), a simple organic compound whose crystalline forms exhibit unexpectedly complex self-assembly behavior.[1,2] Remarkably, phases 1 and 2 represent the first reported occurrence of Frank-Kasper (FK) phases in small organic systems – FK are a class of highly ordered crystalline structures previously observed only in metal alloys [3] and soft matter. These two FK structures crystallized from a dense liquid phase (DLP) formed after liquid-liquid phase separation.

To further investigate the crystallisation behavior of simple salts capable of forming complex phases, we studied systems in which the cation was replaced with imidazolium or the anion with F⁻ or Br⁻. Solution-state NMR experiments were performed at varying concentrations until crystallisation occurred. The cations were probed using ¹H, ¹³C, and ¹⁴N NMR, while ¹⁹F, ^{35/37}Cl, and ^{79/81}Br experiments were employed to investigate the corresponding anions. Selected NOESY and ROESY spectra were compared with classical molecular dynamics simulations of the DLP to gain insight into solute—solvent interactions and pre-nucleation structures. These results provide new perspectives on the role of specific interactions needed to obtain complex crystal architectures from simple molecular precursors.

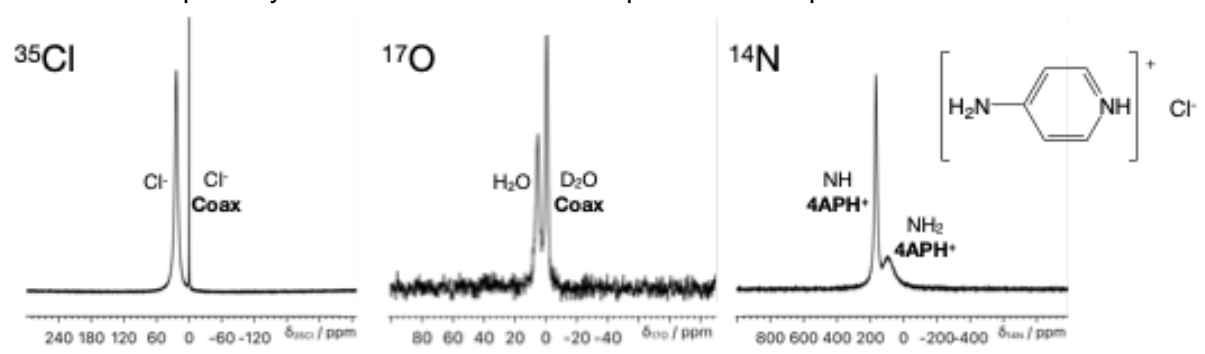


Fig. 1. ³⁵Cl, ¹⁷O, and ¹⁴N NMR spectra of DLP samples of fampridine-HCl, collected immediately after the LLPS, adapted from [2].

- [1] R. Montis, L. Fusaro, A. Falqui, G. Coquerel et al. Nature 590, 275–278 (2021)
- [2] L. Fusaro, N. Tumanov, G. Saielli and R. Montis. *Pure and Applied Chemistry* **95**, 1043–1057 (2023)
- [3] F.C. Frank, & J.S. Kasper, Acta Crystallogr. 11,184-190 (1958).

Beware of the structure: Insights into the Phosphorus Dynamics of postsynthetically modified NU1000 in the presence of water

<u>J. Theissen</u>^{1,2}, E. Derveaux², R. Narvaez³, S. Smeets², N. Gys¹, P. Adriaensens², W. Marchal², R. Ameloot¹

Understanding the structure and chemistry of materials at the atomic scale is essential to elucidate and rationalize their properties as a key step to boost their application in future technologies. Metal-organic frameworks (MOFs) are porous coordination polymers formed by the ensemble of metal ions or clusters and organic linkers, offering a large versatility and tunability in surface area, pore structure, chemical composition, and thermal stability. These properties are attractive for various applications, including gas storage and separation, catalysis and sensing [1]. These applications can be explored by introducing new chemical entities into the MOF framework by metal node functionalization via solvent-assisted ligand incorporation (SALI). In this study, we investigate the post-synthesis modification of the Zr metal node in NU-1000 MOF by reaction with phenylphosphonic acid (PhPA), yielding the material NU-1000-PhPA (Figure 1).

To probe the dynamic behaviour of this modified material in response to water, the material was stored under three different storage conditions and we performed solid-state ³¹P-MAS NMR and two-dimensional dipolar heteronuclear correlation (HETCOR) experiments over an 8-week period. ³¹P-MAS experiments provided valuable insight into the local phosphorus environment, enabling a detailed analysis of the evolution of the structure under different hydration conditions. It allowed us to distinguish between different phosphorus coordination modes and regions within the MOF where water and hydrogen bonding is either present or absent, depending on the loading of PhPA.

This study highlights the advantages of 2D dipolar HETCOR NMR techniques in elucidating the structural changes and coordination environments within MOFs, providing deeper insights into the role of water in modulating material properties over time.

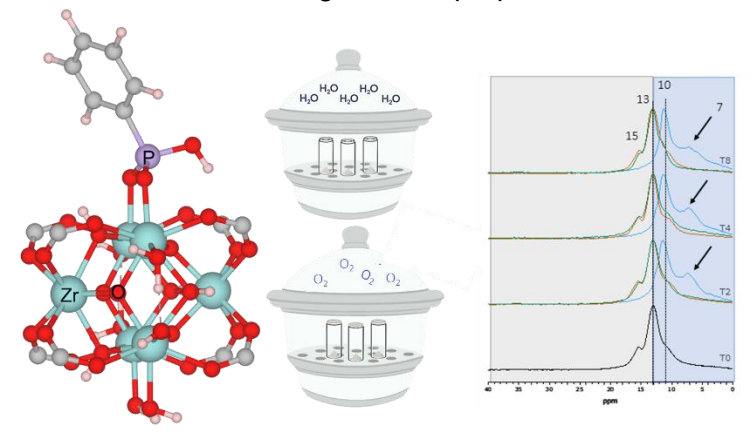


Figure 4: : Graphical representation of the phosphonate grafting on the Zr₆ node of NU-1000 and solid-state ³¹P MAS NMR for different storage conditions, enabling to distinguish the chemical environment in correlation with water.

- 1. Gagnon, K. J., et al., Chemical reviews, 2012, 112 2012, 1034-1054
- 2. Deria, P. et al. Inorg. Chem., 2015, 54, 2185-2192.

¹ Center for membrane separations, adsorption, catalysis, and spectroscopy (cMACS), KULeuven.

² Institute for Materials Research (IMO-IMOMEC), Analytical and Circular Chemistry (ACC), UHasselt.

³ General Chemistry (ALGC) - Materials Modelling Group, Vrije Universiteit Brussel.

Structural Insights into Acyl Chain-Dependent Membrane Interactions of Pseudomonas Cyclic Lipodepsipeptides

Xinyu Qian ^a, Durga Prasad ^a, Annemieke Madder ^b, José C. Martins ^a

^a NMR and Structure Analysis Research Group, and ^b Organic and Biomimetic Chemistry Research Group, Department of Organic and Macromolecular Chemistry, Faculty of Science, Ghent University, Belgium

Cyclic lipodepsipeptides (CLiPs) are secondary metabolites synthesized non-ribosomally by bacteria from various genera, including *Pseudomonas*. They display diverse biological functions that support the lifestyle of their producers, most notably antimicrobial and antifungal activities, making them attractive for agricultural and pharmaceutical applications. CLiPs are particularly remarkable for their chemical diversity, which arises from the ability of non-ribosomal peptide synthetases (NRPSs) to incorporate D-amino acids. They also feature a C-terminal macrocycle formed through ester bond formation between the C-terminus and an earlier hydroxyl containing serine or threonine side-chain. Structurally, most CLiPs adopt a single left handed α_L-helical folds, stabilized in stapled or "golf-club" structural motifs.

In our group, the three-dimensional structures of multiple CLiPs have been determined by NMR spectroscopy, providing a strong foundation for investigating how these molecules interact with membranes. Here, we focus on Orfamide and Viscosin, two closely related CLiPs consisting of 10 and 9 amino acids, respectively. Previous structure–activity relationship studies have shown that, despite their similar peptide sequences, these two CLiPs require different acyl chain lengths to exert membrane-disrupting activity. This suggests that the oligopeptide domain may play a role in defining the optimal chain length. To investigate this, we employed NMR spectroscopy with ¹⁵N labeled Orfamide and Viscosin, obtained from growing the bacteria in minimal media with suitable ¹⁵N sources. Paramagnetic relaxation enhancements (PRE) based on amide NH T1 relaxation rates were measured using ¹H-¹⁵N HSQC for both CLiPs to map the location and orientation of their structures in DPC micelles. Comparative analysis of the experimental data reveals similar trends in the α -helical region of the oligopeptide domain but significant differences for the terminal residues of the macrocycle. Complementary molecular dynamics (MD) simulations in DPC micelles further assessed the hydration shell around amide residues, with computational results in line with the experimental findings.

In future work, more detailed investigations will be carried out to further elucidate the similarities and differences in the interactions of Orfamide and Viscosin with membranes, ultimately aiming to provide a deeper understanding of their mode of action.

Keywords: Cyclic lipodepsipeptides, NMR spectroscopy, Paramagnetic relaxation enhancements, Pseudomonas

